Published in final edited form as:

Annu Rev Biomed Eng. 2013 ; 15: 253–282. doi:10.1146/annurev-bioeng-071812-152409.

Multifunctional Nanoparticles for Drug Delivery and Molecular Imaging

Gang Bao[1], **Samir Mitragotri**[2], and **Sheng Tong**[1]

[1]Department of Biomedical Engineering, Georgia Institute of Technology and Emory University, Atlanta, Georgia 30332

[2]Department of Chemical Engineering, University of California-Santa Barbara, Santa Barbara, California 93106

Abstract

Recent advances in nanotechnology and growing needs in biomedical applications have driven the development of multifunctional nanoparticles. These nanoparticles, through nanocrystalline synthesis, advanced polymer processing, and coating and functionalization strategies, have the potential to integrate various functionalities, simultaneously providing (*a*) contrast for different imaging modalities, (*b*) targeted delivery of drug/gene, and (*c*) thermal therapies. Although still in its infancy, the field of multifunctional nanoparticles has shown great promise in emerging medical fields such as multimodal imaging, theranostics, and image-guided therapies. In this review, we summarize the techniques used in the synthesis of complex nanostructures, review the major forms of multifunctional nanoparticles that have emerged over the past few years, and provide a perceptual vision of this important field of nanomedicine.

Keywords

inorganic nanoparticle; multifunctional nanoparticle; molecular imaging; drug delivery; cancer therapy

TERMINOLOGY

For simplicity, the term nanoparticle, as used in this review, refers to all particulates with at least one dimension falling within 1–100 nm, regardless of their shape or structure. Inorganic nanoparticles have two common structural features: crystalline cores and capping molecules to stabilize these particles in solvents. We use the term nanocrystal to refer to those crystalline cores.

Correspondence to: Gang Bao.

DISCLOSURE STATEMENT

The authors are not aware of any affiliations, memberships, funding, or financial holdings that might be perceived as affecting the objectivity of this review.

INTRODUCTION

The past ten years have witnessed significant advances in nanobiotechnology. A number of nanoparticle-based products for diagnostics and therapeutics have been approved for clinical applications, and even more are currently under clinical trials (1–4). However, the horizon of nanomedicine is still undergoing rapid expansion. An important trend is the development of multifunctional nanoparticles—nanoparticles that are capable of accomplishing multiple objectives such as imaging and therapy or performing a single advanced function through incorporation of multiple functional units. The emergence of these nanoparticles stems from advances in nanofabrication techniques (5–8). With basic nanoparticle synthesis becoming routine, materials scientists are looking into the conception of nanostructures with higher complexity from an engineering perspective (9, 10). This field is also being pushed forward by growing medical needs. For example, the heterogeneity of cancers necessitates image-guided therapies, in which personalized disease treatments are planned based on individual patients' pathological conditions and responses to the treatment (11). This therapeutic regimen has fostered the development of theranostic nanoparticles that integrate diagnosis, drug monitoring, targeted delivery, and controlled drug release into a unifying platform. Furthermore, nanoparticles with multimodal imaging capabilities can offer better images at multiple length scales or treatment stages, facilitating more accurate disease diagnosis and prognosis. Although still far from nanorobots, these multifunctional nanoparticles have the potential to function in a more interactive way, offering invaluable guidence for disease intervention. By revolutionizing conventional medical practices, multifunctional nanoparticles are well poised to shift the paradigm of modern medicine.

An important class of nanoparticles comprises those made of inorganic materials such as metal, metal oxide, and semiconductor, as well as rare earth minerals and silica. These nanoparticles often possess unique electric, magnetic, optical, and plasmonic properties due to the quantum mechanical effects at nanometer scales (12). Thanks to the progresses in nanocrystal synthesis during the past decade or so, most nanoparticles can be generated with a great deal of control over size, shape, and composition, as well as physical properties (6, 13–15). Indeed, many inorganic nanoparticles are now commercially available in various forms. Several types of inorganic nanoparticles are multifunctional by nature. For example, gold nanoparticles are remarkable contrast agents for optical imaging, photoacoustic (PA) imaging, and computed tomography (CT) (16, 17). In addition, gold nanoshells and nanocages can be employed for photothermal therapies (18, 19). It takes only minimal optimization to concurrently utilize imaging and therapeutic features from the same gold nanoparticles. To date, a library of surface chemistry and surface modification techniques are well established for inorganic nanoparticles. Small molecules, including dyes, therapeutic agents, and targeting ligands, can be conjugated to nanoparticles using well-controlled chemistry. More importantly, nanocrystals can be readily decorated with several generic coating strategies, including silica/mesoporous silica, micelle, liposome, and layer-by-layer assembly of biopolymers. These coating methods are useful for both physical/chemical adsorption of small molecules at substantial payload ratios and encapsulation of multiple nanocrystals. As such, numerous multifunctional nanoparticles can be generated by combining existing nanoparticles with small molecules (Figure 1).

Another class of nanostructures being actively explored for therapeutic and imaging applications is organic nanoparticles (20–23). Nanoparticles of different sizes have been prepared using various biodegradable polymers, for example, polylactide-polyglycolide and polycaprolactones, as well as proteinaceous materials, for example, albumin and collagen (24, 25). A variety of therapeutic agents including small molecules, peptides, proteins, and nucleic acids have been encapsulated in these nanoparticles and used for controlled release as well as targeted delivery (26, 27). Imaging contrast agents such as magnetic nanoparticles have also been successfully encapsulated in polymer nanoparticles to enhance circulation and targeting (28, 29). Lipids have been extensively used to prepare drug delivery carriers, especially in the form of liposomal systems. One liposomal system, DOXIL® (doxorubicin), is already being used for the treatment of AIDS-associated Kaposi's sarcoma (30). Protein nanoparticles have found clinical applications for delivery of chemotherapeutic agents (31, 32). ABRAXANE®, a 130-nm, albumin-bound paclitaxel, has been approved by the US Food and Drug Administration (FDA) for the treatment of breast cancer in patients who have failed combination chemotherapy for metastatic disease or who relapse within six months of adjuvant chemotherapy (33). Solid lipid nanoparticles have also been extensively developed for drug delivery applications (34). These particles feature high surface area, favorable zeta potential, and prolonged release of encapsulated drugs (35). Dendrimers are actively used for drug delivery because their properties can be precisely controlled (36). Hydrogels represent another class of materials that are commonly explored for drug delivery owing to their diversity and biocompatibility. Hydrogels, prepared from either natural or synthetic polymers, for example, poly(ethylene oxide) (PEO), poly(vinyl pyrrolidone), or poly-*N*-isopropylacrylamide, have been extensively studied for controlled release and stimuli-responsive release of drugs (37, 38).

This review is propelled by the need to recapitulate current research on multifunctional nanoparticles and stimulate new concepts for the future development of nanomedicine. Owing to space limitations, this review is focuses primarily on inorganic nanoparticles, although a brief overview of organic nanoparticles is provided for completeness. Readers are referred elsewhere for comprehensive reviews of organic nanoparticles (20, 39–44). In the following sections, we briefly review the physical properties and potential applications of nanoparticles and summarize the synthesis strategies used for generating composite nanoparticles. We discuss three promising schemes of multifunctional nanoparticles: combining two or more imaging functions for multimodal imaging, integrating imaging with drug delivery for image-guided drug delivery, and combining drug delivery with thermal therapies to take advantage of synergistic effects. Current clinical trials and future perspectives concerning the application of multifunctional nanoparticles are also discussed.

NANOPARTICLE TECHNOLOGIES—PHYSICAL PROPERTIES AND POTENTIAL APPLICATIONS

Gold Nanoparticles

The most common type of gold nanoparticles is gold nanosphere, which exhibits an intense ruby color in aqueous solutions. The intriguing optical properties of gold nanoparticles arise from localized surface plasmon resonance (LSPR), in which valence electrons in gold

nanoparticles oscillate coherently with incident light at specific frequency (45). Part of the energy absorbed by gold nanoparticles is emitted in the form of scattered light, which is the basis of much gold nanoparticle–based optical imaging (46). The rest of the energy decays in a nonradiative form; that is, it is converted into heat. Gold nanospheres within a wide size range absorb light mainly at around 520-nm wavelength, at which light is rapidly attenuated by the tissue. For in vivo applications, the absorption peak should fall within the optical window of human tissues (650–1300 nm) so that the incident light can penetrate deep into tissue (47). The absorption spectrum of gold nanoparticles can be tuned through their geometry (48). For example, in gold nanorods, LSPR occurs in two directions: along the short- and the long-axes. The frequency of oscillation along the long axis redshifts from the visible to the near infrared (NIR) region as the aspect ratio of the nanorods increases (19). Other gold nanostructures with tunable LSPR frequency are gold nanoshells and nanocages, the absorption spectra of which change with the overall size and thickness of their walls (Figure 2*a*) (49, 50). Aggregated gold nanospheres may also exhibit significant NIR absorption as a result of coupled plasmon resonance. This phenomenon has often been used to create nanostructures with NIR photothermal properties for in vivo applications (51).

Gold nanoparticles scatter light strongly at their LSPR frequency and thus have broad applications in optical imaging (52). Futhermore, gold nanoparticles increase local electromagnetic field because of LSPR. As a result, the signals of fluorophores and SERS (surface-enhanced Raman scattering) reporters attached to a gold surface can be drastically enhanced (53). In in vivo applications, gold nanoparticles that scatter NIR light can provide good contrast for optical coherence tomography (17). Alternatively, gold nanoparticles with NIR photothermal properties are ideal probes for photothermal therapy (18). This photothermal property also makes gold nanoparticles excellent contrast agents in PA imaging (54). Recent studies have shown that gold nanoparticles can be heated by nonresonant shortwave radiofrequency fields, which allows the induction of targeted hyperthermia in deep tissue (55). Lastly, gold nanospheres and gold nanorods have been used as contrast agents in CT, taking advantage of the element’s high material density and high atomic number (16, 56).

Magnetic Nanoparticles

Magnetic nanoparticles are composed mainly of iron oxides (magnetite and maghemite) and to a lesser extent of elementary iron and other magnetic elements (14, 57). When the size of magnetic particles is smaller than the magnetic domain wall width (typically less than 100 nm), the particles will contain only a single magnetic domain with the magnetic moment from all unpaired electrons coupled in one direction (58). The coupled magnetic moment flips among several crystal axes of the nanoparticle owing to thermal fluctuation. When the particle size further decreases, the flipping rate increases rapidly until no net magnetization can be observed. The magnetic nanoparticles within this size limit are called superparamagnetic nanoparticles. The superparamagnetic limit of iron oxide nanoparticles is between 20 and 25 nm at room temperature (58). Without external magnetic field, neighboring superparamagnetic nanoparticles are free of interparticle magnetic interactions, which is critical for the colloidal stability of the nanoparticles. However, when an external magnetic field is applied, the magnetic moment of the nanoparticles will align with the field

and reach saturation at relatively low field strength. Magnetite and maghemite, owing to their excellent biocompatibility, are the most common types of materials used in magnetic nanoparticles. Nanoparticles of materials that have higher saturation magnetization, including elementary iron, cobalt, and iron oxide doped with manganese and zinc, have also been developed (Figure 2*b*) (59, 60).

Superparamagnetic iron oxide nanoparticles (SPIOs), as either a T_1 or a T_2 contrast agent for MRI, have the potential to significantly improve the sensitivity of clinical tumor detection (61). T_2 relaxivity of magnetic nanoparticles is determined by their magnetic moment and coating conformation (59, 62). In general, magnetic nanoparticles with higher magnetization, large core, and thin surface coatings have higher T_2 relaxivity. In particular, SPIOs with large size and high magnetization can have T_2 relaxivity two orders of magnitude higher than that of clinically approved first-generation SPIOs on a per particle basis (62). These nanoparticles hold great promise in MRI-based molecular imaging. In addition, the T_2 relaxivity of magnetic nanoparticles increases upon aggregation, a phenomenon referred to as magnetic relaxation switching (63). Accordingly, an approach for achieving high T_2 relaxivity is to generate nanoparticles with multiple magnetite cores (64).

In the past few years, magnetic nanoparticles have garnered extensive research interest with respect to hyperthermia induction and magnetic targeting. Magnetic nanoparticles can generate heat under an oscillating magnetic field (100 kHz to 1 MHz), which enables the induction of hyperthermia in deep tissue (65–67). Magnetic targeting has been widely used in various in vitro applications, including cell separation, gene transfection, and sample enrichment in detection assays. Recent studies show that in vivo magnetic targeting can be a valuable approach for controlled delivery of therapeutic agents (68, 69). The magnetic mobility and heating capability of magnetic nanoparticles can also be employed to trigger cellular events in vivo (70, 71).

Quantum Dots

Quantum dots (QDs), essentially fluorescence-emitting semiconductor nanoparticles, have attracted extensive study in optical imaging during the past decade (72). Most QDs are composed of binary alloys of II–VI (e.g., CdSe) or III–V (e.g., InP) semiconductor materials. To improve the quantum yield, QDs are often encapsulated in an insulating inorganic shell (e.g., ZnS). The optical properties of QDs are the result of quantum confinement of valence electrons at nanometer scales (12). The fluorescence emission wavelength is dictated by the energy band gap determined by QD size and composition (Figure 2*c*) (73). The emission peak redshifts as the size of QDs increases. In contrast to organic fluorophores, QDs have a narrow emission peak and an absorption spectra ranging from UV to visible wavelengths. Therefore, multiple QDs with different emission wavelengths can be excited simultaneously upon UV excitation, facilitating multicolor fluorescence imaging. Recently, owing to their NIR excitation and emission, QDs composed of CdTe, PbS, InAs, and InP have attracted broad interest for in vivo applications. Concerns over the in vivo toxicity of heavy metals have also prompted searches for biocompatible QDs (74).

Upconversion Nanoparticles

The development of small upconversion nanoparticles (~10 nm) has become possible only in the past few years, following advances in rare-earth nanoparticle synthesis (75). In contrast to QDs, upconversion nanoparticles can absorb infrared radiation and emit photons at visible spectra. This upconversion process is achieved through continuous excitation of valence electrons of lanthanide ions by photon absorption or energy transfer from nearby excited lanthanide ions (76). These nanoparticles are composed of a host material doped with lanthanide ions that act as sensitizers (Yb^{3+}) and activators (Er^{3+}, Tm^{3+}, and Ho^{3+}). The absorption and emission peaks of upconversion nanoparticles are very narrow, resembling those of free lanthanide ions. Similar to QDs, upconversion nanoparticles have an emission spectrum that can be tuned within a wide range by changing host materials, sensitizer ions, and doping density. (Figure 2*d*) (75, 77).

Upconversion nanoparticles can be excited with low-power, continuous wave laser, as opposed to conventional two photon excitation in optical imaging, because the upconversion process is based on physically existent energy states of lanthanide ions. To date, upconversion nanoparticles are excited mostly at 980 nm using a commercial InGaAs diode laser system. The low-power NIR excitation makes upconversion nanoparticles particularly useful for in vivo optical imaging. Not only can the infrared light penetrate deep into the tissue, but auto fluorescence from the tissue is also greatly reduced. Upconversion nanoparticles can form fluorescence resonance energy transfer (FRET) pairs with organic fluorophores or photosensitizers. Indeed, coupling upconversion nanoparticles with photosensitizers resulted in increased efficiency and working depth in cancer photodynamic therapies (78).

Other Inorganic Nanoparticles

There are many other types of inorganic nanoparticles, including silica nanoparticles (79), calcium phosphate nanoparticles (80), carbon nanotubes, and hafnium oxide nanoparticles (81). Silica and calcium phosphate nanoparticles do not exhibit unique quantum mechanical properties. However, they offer great biocompatibility, convenient size tuning, rich conjugation chemistry, and versatile cargo loading schemes. These nanoparticles are broadly used as carriers of drug molecules, genes, and imaging contrast agents (82–84). Silica nanoparticles carrying organic dyes and radioactive iodide, known as Cornell dots or C dots, have been approved for clinical trials. Nanoparticles formed by hafnium oxide can significantly enhance the efficiency of X-ray in radiation therapy; they are also undergoing phase I clinical trials.

Polymeric Particles

Polymeric particles are among the most widely explored organic nanoparticles. They offer several advantages, including the ability to (*a*) encapsulate a wide variety of drugs and release them over prolonged periods, (*b*) modify surfaces with multiple targeting ligands, and (*c*) exhibit excellent stability, both in vitro and in vivo. Polymeric materials have a long history of use in medicine, including for drug delivery (85). Biodegradable polyesters such as poly(lactic acid) (PLA), poly(glycolic acid), and their copolymers as well as poly(ε-caprolactone) have been explored for various drug delivery applications (86). Other

biodegradable polymers used for nanoparticle synthesis include poly(orthoesters) and poly(anhydrides), among others (24). Copolymers of hydrophobic polymers, such as those listed above, with hydrophilic polymers such as poly(ethylene glycol) (PEG), PEO, and poly(propylene oxide) (PPO) are used to synthesize self-assembled therapeutic carriers (87). Responsive polymers (88)—that is, materials that respond to an external stimulus such as temperature, pH, or electromagnetic radiation—are also actively explored in drug delivery (89–94).

SYNTHETIC STRATEGIES OF MULTIFUNCTIONAL NANOPARTICLES

Despite the large difference in inorganic nanoparticle's chemical compositions, their synthetic methods share many similarities. The formation of most inorganic nanoparticles involves two phases: nucleation and crystal growth by deposition of atoms on the crystal surface. QDs, iron oxide nanoparticles, and upconversion nanoparticles can be synthesized through coprecipitation or thermal decomposition of precursor compounds with similar capping molecules and solvents (57, 75, 95, 96). In the past few years, several generic coating methods have become well established for inorganic nanocrystals. Polymers can be grafted onto most crystal surfaces through metal coordination or chelation (97–100). Hydrophobic nanocrystals can be readily encapsulated with a layer of amphiphilic copolymer such as poloxamer, poloxamine, or lipid-PEG (101–103). Nanocrystals with strong surface charge can be coated with polyions through layer-by-layer assembly (104). In addition, silica or mesoporous silica coating methods have been demonstrated for most hydrophilic and hydrophobic nanocrystals (105, 106). These common synthetic routes facilitate the integration of different nanoparticles or the combination of nanoparticles with small molecules carrying a wide range of functions (Table 1).

Nanoparticle-Nanoparticle Assembly

A direct approach to combining two different nanoparticles is seed-mediated growth, in which one type of nanoparticle is synthesized with another type as the seeds. For example, a layer of $NaGdF_4$ can grow on $NaGdF_4$:Yb^{3+}/Er^{3+} nanocrystals, resulting in nanoparticles with combined upconversion and T_1 properties (107). Dumbbell-like gold-iron oxide nanoparticles can be synthesized by thermodecomposition of iron precursors in the presence of gold nanoparticles (108). Likewise, gold nanoshells can be formed by directly reducing gold salts onto the surface of exogenous nanocrystals. Au@Fe and Au@Fe_3O_4 nanoparticles have been obtained using this method (15, 109). Many nanocrystals can grow on silica surfaces, including the surface of silica nanospheres or nanocrystals with a silica coating. For this reason, a layer of silica has often been used to bridge two different crystals (110).

Nanoparticles can be combined through postsynthesis assembly. Metal atoms exposed on the nanocrystal surface can form stable bonds with chemical groups such as -SH, -OH, -COOH, and -NH_2 through metal coordination or chelation. This has often been used to deposit small nanocrystals to the surface of a large nanoparticle. For example, small gold nanospheres can be adsorbed onto an amine-rich surface of silica or iron oxide nanoparticles (18, 111–113). Subsequently, a continuous gold shell can grow on the central nanoparticle by filling the gap among the gold nanospheres with further reduction of gold salts (18, 111, 112). A cluster of

nanoparticles can also form through chemical/biological bonds among surface-coating molecules (112, 114).

As-synthesized nanocrystals can be combined together through controlled self-assembly due to hydrophobic or electrostatic interactions. Small clusters of hydrophobic QDs and SPIOs can be encapsulated with a layer of amphiphilic copolymer such as lipid-PEG or PEG-PLA (115, 116). QDs with negative charges can form aggregates when mixed with PEG-poly(ethyl enimine) (PEI) (117). Multiple nanoparticles can also be simultaneously enclosed in liposomes during assembly of lipid bilayers (69). Furthermore, hydrophobic nanoparticles can be confined through reverse microemulsion, after which mesoporous silica nanoparticles form (118). As a result, each mesoporous silica nanoparticle can contain several types of nanocrystals.

Nanoparticle–Small Molecule Assembly

Small-molecule cargos commonly added to nanoparticles include dye molecules, radioisotopes, drug molecules, siRNA/miRNA, peptides, and targeting ligands. Depending on the functional requirements, these molecules are loaded at different quantities at the center or the surface of nanoparticles. The methods for nanoparticle–small molecule assembly can be divided into two categories: chemical conjugation and physical adsorption.

Most molecules can be directly conjugated to coating molecules or polymer scaffolds on the nanoparticle surface (82, 119, 120). The signal intensity of fluorophores and SERS reporters can be affected by conjugation chemistry, loading density, and the distance to the nanocrystal (53, 82). For drug molecules, it is critical to reach concentrations above a therapeutic threshold in the target tissue. Accordingly, drug molecules should be loaded onto nanoparticles at a high payload ratio and released from nanoparticles at a proper rate after reaching the target tissue. For this reason, drug molecules are often conjugated to nanoparticles through molecular linkers that can be degraded by enzyme cleavage, hydrolysis, or heating. It is also possible to release drug molecules based on pH changes.

Small molecules can be encapsulated in micelles, liposomes, mesoporous silica, or nanotubes through hydrophobic interaction, electrostatic interactions, or physical entrapment (115, 121–123). Encapsulated molecules can be released after disassembly of the nanoparticles triggered by cellular uptake or external signals. Small nucleic acids, owing to their negative charge, are often adsorbed to nanoparticles via electrostatic interactions (124, 125).

Polymer Particles

Polymer nanoparticles are traditionally prepared using methods including solvent evaporation, spontaneous emulsification, solvent diffusion, salting out/emulsification-diffusion, and use of super critical CO_2, among others (86). Polymeric nanoparticles ranging in size from a few nanometers to hundreds of nanometers or larger have been prepared using these methods. Nanoparticles less than 200 nm in diameter have been particularly appealing for intravascular drug delivery applications because they show improved circulation half-life as compared with larger particles (126, 127). Polymer nanoparticles are often coated with a hydrophilic polymeric brush, typically PEG, to prolong circulation and avoid clearance by

the mononuclear phagocytic system (128). Polaxamers and polaxamines and hydrophilic-hydrophobic block copolymers have also been extensively studied for this purpose (87, 129). Simultaneous coating of a nanoparticle surface with peptides (130, 131), aptamers (132–134), and antibodies (135, 136) has also been explored to enhance targeting. Striking a balance between immune evasion by PEG and targeting by peptides is often essential. Accordingly, strategies have been developed to optimize surface concentrations of PEG and targeting ligands by random distribution of PEG and aptamers on the nanoparticle surface (137) and by fabrication of compartmentalized particles that allow stereospecific coating with various chemical groups (7, 138). Recently, the importance of nanoparticle mechanical properties in therapeutic functions has been highlighted. Specifically, it has been shown that macrophages engulf rigid particles to a significantly higher extent than soft particles (139), a finding that has implications in immune clearance of nanoparticles. Recent studies have also shown that the shape of nanoparticles can have an intriguing effect on their function (13, 140–146). Several methods have been developed to synthesize organic particles of different shapes (8, 140, 147, 148). Nonspherical nanoscale particles of various shapes, including rods and discoids, have been fabricated using the top-down Particle Replication in Non-wetting Templates (PRINT®) technology (140, 149). Methods have also been put forth to synthesize nanoparticles with various internal architectures (150). This feature is especially important in the incorporation of multiple agents, for example, imaging and therapeutic agents, within a single nanoparticle. Electrohydrodynamic cojetting has been used to prepare biphasic and triphasic nanoparticles that are able to encapsulate agents of various diverse physical-chemical properties (7).

NANOPARTICLES AS IMAGING CONTRAST AGENTS

Medical imaging plays important roles in disease detection, prognosis, and treatment planning. Major medical imaging techniques include X-ray CT, magnetic resonance imaging (MRI), ultrasound imaging, positron emission tomography (PET), single-photon emission CT (SPECT), optical imaging, and PA imaging. The intrinsic quantum mechanical properties of inorganic nanoparticles make them remarkable contrast agents for MRI, optical imaging, and PA imaging, and by incorporating small molecules, these nanoparticles can be used in nearly all imaging modalities.

Magnetic Resonance Imaging

MRI is a nonionizing imaging technique that produces excellent signal contrast for soft tissue by detecting the nuclear spin of hydrogen atoms, which predominantly come from water and fat in a human body. MRI contrast agents can provide bright or dark contrast by accelerating either T_1 or T_2 relaxation of water protons, respectively. Most magnetic nanoparticles, such as SPIOs, are designed as T_2 or T_2* contrast agents. In T_2-weighted MRI, the tissue containing SPIOs exhibits reduced signal intensity. In recent years, alternative MRI pulse sequences have been devised to produce positive contrast from magnetic nanoparticles (151, 152). Magnetic nanoparticles including gadolinium and manganese nanoparticles, as well as SPIOs with small T_2/T_1 ratio (e.g., Resovist®), can also provide bright contrast in T_1-weighted MR images (153).

The use of SPIOs as contrast agents has greatly expanded the application of MRI in disease diagnosis, owing to the high T_2 relaxivity and biocompatibility of these nanoparticles. After being administrated systemically, dextran-coated SPIOs, such as Feridex I.V.®, can accumulate in liver as a result of phagocytosis by the reticuloendothelial system (RES). Liver tumors' lack of phagocytic activity can thus be detected by the darkening of surrounding normal tissue (61). This method is also applied for detecting splenic tumors and metastatic lymph nodes (154). Two types of SPIOs, Feridex I.V. and Resovist, have been approved by the FDA for clinical application and are the first inorganic nanoparticles on the market. SPIOs can also accumulate in the tumor by enhanced permeability and retention (EPR) effects, which facilitates tumor detection in tissues or organs that normally do not sequester SPIOs from blood circulation.

More recently, SPIOs with high T_2 relaxivity have been explored for in vivo molecular imaging of disease markers and physiological processes. For example, SPIOs conjugated with targeting ligands can detect atherosclerotic plaques, tumors, and apoptotic tissues (59, 64, 155–158). SPIO nanosomes functionalized with apolipoprotein E and lipoprotein lipase were used to study lipoprotein metabolism in liver (159). In a study by Kessinger et al. (160), T_2*-weighted time-resolved MRI was used to study the binding kinetics of superparamagnetic micelles to $\alpha_v\beta_3$-integrin expressed on the tumor vessel surface, demonstrating the potential of magnetic nanoparticles in quantitative analysis of disease markers in vivo.

SPIOs have also been extensively used for in vivo cell tracking. Tracking immune cells labeled with an SPIO has been an important approach in detecting atherosclerosis (161). In regenerative medicine, there is a great need for noninvasively examining the in vivo distribution of implanted cells. Studies have shown that progenitor cells can be labeled with many SPIOs without affecting cell viability or function (162, 163). After being injected intravenously, the cells located in bone marrow could be detected at high resolution (162). In a similar application, pancreatic islet cells were loaded into magnetocapsules containing Feridex I.V. (164). The hepatic distribution of infused magnetocapsules was readily examined with MRI in vivo.

In Vivo Optical Imaging

Compared with other medical imaging modalities, optical imaging has excellent spatial resolution and detection sensitivity in cellular imaging (reviewed elsewhere). However, its in vivo applications are hindered by autofluorescence of tissue and light attenuation. Owing to limited tissue penetration, optical imaging, almost exclusively NIR imaging, is used mainly to examine shallow lesions and superficial objects, including subcutaneous or surgically exposed organs, tumors, sentinel lymph nodes, and lymphatic vessels, as well as retinal and choroidal vasculatures (165).

Nanoparticles designed for optical imaging include QDs, upconversion nanoparticles, gold nanoparticles, and nanoparticles containing organic dyes. Kim et al. (166) first demonstrated that NIR QDs (CdTe core/CdSe shell) could be used to map sentinel lymph nodes in mouse and in pig. Importantly, in the large-animal model, lymph nodes that are 1-cm deep could be readily identified following intradermal injection of 400 pmol of NIR QDs. More recently,

Ag_2S QDs free of heavy metals (Cd, Hg, or Pb) were developed for the NIR-II imaging (wavelength of 1,000–1,400 nm) (74, 167). PEGylated Ag_2S QDs showed good tumor detection sensitivity through passive tumor targeting in a mouse model (74). C dots, a class of silica nanoparticle mentioned above, are representative of nanoparticles containing organic fluorophores (82). Fluorophores conjugated to the silica matrix exhibit a more than twofold increase in quantum efficiency (82). C dots containing Cy5 dyes were used to visualize lymphatic drainage from the peritumoral region, and detailed intranodal architecture could be identified at submillimeter scale in high-resolution fluorescence images (119). Although the application of upconversion nanoparticles in in vivo imaging is still at an early stage, a few proof-of-concept studies have shown an outstanding potential of upconversion nanoparticles owing to their long wavelength excitation (168, 169). Gold nanoshells and nanocages that scatter light in the NIR region can enhance optical coherence tomography (OCT) (17, 170). For example, Gobin et al. (17) showed that gold nanoshells injected systemically could significantly enhance the contrast ratio of the tumor to the normal muscle in OCT.

Photoacoustic Imaging

PA imaging is a new imaging modality that combines optical and ultrasound imaging techniques. It offers far better tissue-penetration depth (~50–70 mm) than does optical imaging and maintains decent spatial resolutions (171). In PA imaging, contrast agents convert incident light into heat. Subsequently, the heat causes thermoelastic expansion of surrounding medium- and wideband ultrasound emission that can be detected with ultrasound transducers. For in vivo applications, the contrast agents should be able to absorb light at the NIR region and efficiently convert absorbed energy to heat. These properties are identical to those required in photothermal therapies. For this reason, most nanoparticles that were initially developed for photothermal therapies have been tested for PA imaging as well.

Gold nanoparticles, including nanospheres, nanoshells, nanorods, and nanocages, can be used as contrast agents in PA imaging (172–174). As blood-pool contrast agents, nontargeting gold nanoshells and gold nanocages enhanced the contrast of vasculature in rat brain (172, 173). Molecular imaging using antibody-conjugated gold nanorods has been demonstrated in culture cells and tissue phantoms (175). Galanzha et al. (176) showed that gold-plated carbon nanotubes conjugated with folic acid could detect circulating cancer cells magnetically enriched in mouse ear. In addition, gold nanospheres conjugated with antibody formed small aggregates on cancer cells (A431 cells) overexpressing epidermal growth factor receptor (EGFR). Aggregation of the gold nanospheres led to a redshift of their absorption spectrum, which could be detected with PA imaging (177). Recently, copper-based nanoparticles and nanoparticles containing NIR dyes were also developed for PA imaging (178–180).

Nanoparticles for Multimodality Imaging

Owing to the limitations in cost, imaging time, resolution, specificity, and detection sensitivity, each imaging technique is effective only for examining one particular aspect of disease or is limited to one stage of the therapeutic intervention. Usually, several imaging techniques are used along the course of disease diagnosis, prognosis, and treatment.

Integrating several imaging techniques into one unifying platform, that is, multimodality imaging, has significant potential for expanding current imaging techniques toward better disease management. Multimodality imaging techniques have been realized through two different, but related, approaches: One is to forge different imaging instruments into one piece; the other is the development of multimodal imaging agents. Most multimodal imaging agents are derived from nanoparticles because of the ease of synthesis and functionalization. The nanoparticles designed for MRI, optical imaging, and PA imaging described above can be readily conjugated with small-molecule imaging moieties, including fluorophores, SERS reporters, MRI contrast agents (Gd^{3+} or Mn^{2+}), and radiotracers, to form dual- or trimodal imaging probes. Multimodal nanoparticles can often support better spatial registration of different imaging modality and avoid excessive immune responses caused by repeated challenge.

A number of multimodal nanoparticles combine the use of a full body scan with an imaging modality that offers local but high-resolution images. This approach allows characterization of the disease at multiple spatial scales, which is not only helpful in clinical diagnosis and laboratory research but also important for treatment planning. For example, SPIOs labeled with Cy5.5 can be used in both MRI and NIR imaging (181). Coarse tumor location in the brain is identifiable with MRI, and NIR imaging provides precise tumor delineation to guide surgical removal of tumor. Several other types of MRI/optical dual-modality nanoparticles have been developed by combining SPIOs with fluorophores, QDs, or upconversion nanoparticles (106, 107, 115, 118, 182, 183). In a similar approach, gold nanospheres were functionalized with both a Raman molecular tag, *trans*-1,2-bis(4-pyridyl)-ethylene, and an MRI T_1 agent, DOTA-Gd^{3+}, in order to accommodate MRI, PA imaging, and Raman imaging (Figure 3) (184). Following MRI scan, intraoperative resection could be performed in accordance with the brain tumor margins observed through Raman imaging. Furthermore, C dots, discussed above for optical imaging, could be labeled with ^{124}I to enable highly sensitive detection of primary tumors and metastatic lymph nodes with PET (119).

There is a critical need in medical imaging to coregister functional PET images with those offering detailed anatomical structures. Among all medical imaging techniques, PET provides the highest tumor detection sensitivity because of the use of radiotracers. However, tumor sites with high radioactivity cannot be accurately located in the abdomen or near the boundary of a moving organ owing to a lack of anatomical structure in the PET images. For this reason, PET is often performed along with either MRI or CT (182, 185). MRI offers excellent soft-tissue contrast and thus facilitates tumor localization in coregistered MRI and PET images. To date, PET/MRI dual-modality nanoparticles are mainly generated by labeling SPIOs with chelates of ^{64}Cu (186).

NANOPARTICLES AS DRUG DELIVERY VEHICLES

During cancer treatment, therapeutic compounds often need to be delivered into individual tumor cells to exert anticancer effects. However, the molecules administered systemically are typically distributed to the whole body through blood circulation and subjected to hydrolysis, enzymatic degradation, and rapid excretion through the urinary system. Also, the accumulation of these drugs in the tumor is often suboptimal owing to lack of specific

targeting. These issues not only hamper traditional chemotherapy utilizing small hydrophobic drugs but also pose a major challenge to gene therapies aiming to correct aberrant tumor growth with miRNA or siRNA (187). Targeted delivery of drug molecules with nanoparticles can improve biodistribution, increase circulation half-life, and protect drugs from the microenvironment, thus increasing efficacy and reducing side effects.

The study of nanoparticle-based drug delivery systems has been performed mostly with organic nanoparticles (2). This is largely attributable to the better understanding of in vivo metabolism and toxicity of organic materials. In addition, many organic nanoparticles such as liposomes, micelles, and dendrimers can carry drug molecules at a substantial payload ratio that the inorganic nanoparticles discussed above can barely reach. Many excellent reviews that cover the advances of organic nanoparticles and their clinical applications can be found in the literature (39, 188–192).

Recently, the toxicity issue has been largely resolved. Several inorganic nanoparticles have either entered the market or been approved by the FDA for clinical trials. The success in developing liposomal, micellar, and mesoporous-silica coatings for inorganic nanoparticles further overcomes the difficulties in drug loading. Inorganic nanocarriers have since become a hot spot in nanomedicine because of the unprecedented imaging and control capabilities offered by their unique physical properties. Reviewed below are studies in three important areas: image-guided drug delivery, magnetic drug targeting, and combined chemotherapy and thermal therapy.

Image-Guided Drug Delivery

The success of cancer chemotherapy depends on the ability to deliver drug molecules to the entire tumor cell population at concentrations above a therapeutic threshold. It requires that drug molecules not only accumulate at a high level over the whole tumor but also distribute evenly in the tumor stroma. However, vessel density, vessel permeability, and expression of molecular markers, which are key factors in determining drug distribution, often vary among different tumor regions, disease stages, and patients. A standard treatment plan would be effective only during a narrow therapeutic window in a subpopulation of patients. In the burgeoning field of image-guided drug delivery, this issue is addressed by using imaging tools to guide disease interventions according to individual patients' pathological conditions and responses to the treatment.

An important part of image-guided drug delivery is to monitor the biodistribution, blood circulation, and tumor accumulation of drug molecules. For this purpose, several strategies were devised to load drugs onto or into nanoparticles that can be visualized with medical imaging approaches. Among all inorganic nanoparticles, SPIOs are the most popular choice because of their excellent MRI contrast and biocompatibility. Micelles, liposomes, and mesoporous silica containing single or multiple SPIOs have been loaded with chemotherapeutic drugs such as doxorubicin and paclitaxel (106, 115, 116, 193). The resulting SPIO/drug complex can achieve high drug payload while maintaining good MRI T_2 contrast. MRI/NIR dual-modality SPIOs have been used to image in vivo siRNA delivery (Figure 4) (194). In this study, siRNA was conjugated to dextran-coated SPIOs, to which an NIR dye, Cy5.5, was also attached. The accumulation of siRNA in the tumor was visualized

with both MRI and in vivo NIR optical imaging. Cho et al. (195) further showed that SPIOs could deliver tumor antigen to dendritic cells in vivo. The distribution of activated dendritic cells could be tracked through intracellular SPIOs with MRI. Viglianti et al. (196) developed a thermosensitive liposome containing both doxorubicin and $MnSO_4$. The release of $MnSO_4$ monitored with MRI was indicative of the release of doxorubicin. Other detectable nanoscale drug carriers include gold nanorods, gold nanocages, and gold nanoshells. The distribution of these nanoparticles could be examined at high resolution with PA imaging.

Molecular imaging can also provide valuable insight into tumor responses to cancer treatment. For example, the underglycosylated MUC-1 (uMUC-1) tumor antigen is predictive of chemotherapeutic response of breast cancers. Medarova et al. (197) found that the tumoral accumulation of SPIOs targeting MUC-1 was markedly decreased following doxorubicin treatment, indicating a positive response to the chemotherapy.

Magnetic Drug Targeting

The ability to actively control drug distribution in vivo has been constantly pursued in the field of drug delivery. Magnetic targeting has long been considered a viable approach toward this goal. Magnetic nanoparticles, being nanosized magnets, experience a force in an inhomogeneous magnetic field. The magnitude of the force depends on the magnetic moment of the nanoparticles and the gradient of the magnetic field (198). Through proper design of the externally applied magnetic field, therapeutic agents attached to magnetic nanoparticles can be attracted to local tissue under magnetic guidance (199, 200).

In vivo magnetic targeting was first demonstrated with magnetic albumin microspheres (clusters of albumins with magnetite particles of 10–20-nm diameter) in the late 1970s (201). The same microspheres containing doxorubicin were able to induce total remission of Yoshida sarcoma in a rat model (202). Another form of magnetic microparticles, MTC-DOX, also gained initial success for cancer treatment in animal models (203). However, MTC-DOX eventually failed to advance to clinical applications after the termination of phase II/III clinical trials in 2004.

Gradually, the study of magnetic targeting shifted to magnetic nanoparticles, which, compared with microparticles, may offer better biocompatibility, optimal biodistribution, and deeper tumor penetration. Alexiou et al. (204) treated VX-2 squamous cell carcinoma with starch-coated SPIOs bound to mitoxantrone in a hind-limb tumor model of rabbits. Positive outcomes were obtained with intra-arterial but not intravenous injection of SPIO/drug complex, a result which was presumably due to the higher tumor availability of SPIO/drug complex upon intra-arterial injection. Many other types of magnetic nanoparticles, including liposomes-, micelles-, and mesoporous silica–coated SPIOs, have been successful in magnetic targeting of chemotherapeutic drugs in animal models (121, 193). Magnetically guided gene therapy was demonstrated with a positively charged magnetic lipid nanoparticle that could adsorb negatively charged siRNA through electrostatic interaction (69). Magnetic targeting was also able to significantly enhance tumor suppression by EGFR siRNA. Chorny et al. (205) demonstrated that magnetic targeting could be achieved with an implanted magnetic stent. After the stent’s implantation, injection of paclitaxel-loaded magnetic nanoparticles could lead to significant growth inhibition in the stented vessel.

Magnetic targeting can also be applied to larger cargos (68, 206, 207). For example, inhaled magnetic aerosol droplets of 2.5–4-μm diameter could be targeted to the affected lung tissue with a magnetic field (68). In another study, SPIOs were bound to lentiviral vectors through electrostatic interactions (206). Magnetized lentiviral vectors were able to deliver enhanced green fluorescent protein (eGFP) plasmid to magnetically targeted mouse aorta ex vivo (Figure 5). Furthermore, lentivirus/magnetic nanoparticle–transduced endothelial cells could be positioned to injured common carotid artery by magnetic forces. Likewise, cardiac-derived stem cells loaded with iron macrospheres could be sequestrated in the left ventricular cavity with a superimposed magnet in a rat model (207).

Drug Delivery in Combination with Thermal Therapy

It is well known that certain cancers can be treated with hyperthermia. Local heating can significantly increase the extravasation of nanoscale drug carriers from tumor vessels (208). Further, cancer cells at elevated temperatures are more vulnerable to chemotherapy. As a result, combined thermal therapy and chemotherapy often show more pronounced synergistic effect than the sum of the individual therapies. This combination has therefore become a promising paradigm for cancer intervention. Traditionally, the combined therapy relies on two separate treatments, which have to be carefully arranged in order to achieve synchronized effects (208). As mentioned above, gold nanoparticles and magnetic nanoparticles can deliver effective cancer thermal therapies. When loaded with drug molecules, these nanoparticles provide a unifying platform for combined thermal therapy and chemotherapy.

A critical step in the combined therapy is controlled drug release. In this regard, drug molecules are usually stored in structures responsive to heating. Focused heating can therefore trigger transient drug release, resulting in a high local concentration of drug molecules in the target tissue. As shown with nanoparticles consisting of magnetite shell/silica core, heating in an oscillating magnetic field would break the magnetite shell and subsequently release the model drug compounds stored in the silica matrix (209). In a different approach, doxorubicin was loaded in mesoporous silica sealed with thermosensitive nanovalves (Figure 6) (210). Heating of zinc-doped iron oxide nanocrystals encapsulated in mesoporous silica led to rapid drug release.

Heat-triggered release has also been realized for gene delivery. Derfus et al. (211) conjugated double-stranded DNA molecules to dextran-coated SPIOs. Heat applied to an SPIO could induce enough temperature increase to initiate melting and release single-stranded DNA oligos. Lu et al. (212) developed a hollow gold nanoshell conjugated with thiolated siRNA. Interestingly, although the nanoshell could always be internalized into cultured cells, gene silencing occurred only after NIR radiation, indicating NIR light–activated endolysosomal escape of siRNA. In the same study, the investigators further showed in vivo tumor suppression as a result of p65 siRNA photothermal transfection coupled with irinotecan treatment.

CURRENT CLINICAL TRIALS AND FUTURE PERSPECTIVES

The first FDA approval granted to inorganic nanoparticles dates back to the mid-1990s. Since then, a limited number of inorganic nanoparticles have successfully entered the market or clinical trials (Table 2). These inorganic nanoparticles cover a wide range of clinical applications, including three iron oxide nanoparticles (Feridex I.V., GastroMARK™ and Resovist) and one silica nanoparticle (C dots) developed for tumor detection using MRI, optical imaging, and PET. A common feature of these four nanoparticles is that they can be cleared from the body by either degradation or excretion through the urinary system (119). Thermal therapies have attracted much attention in clinical treatment of tumors and atherosclerotic plaques. Thermal ablation of tumor can be achieved by focused radio frequency or NIR radiation following intratumoral injection of SPIOs or gold nanoshells, respectively. Local injection is utilized to obtain high concentration of nanoparticles in the tumor and reduce systemic side effects. Other clinical applications of inorganic nanoparticles include wound healing, drug delivery (TNF-α), and radiation therapy.

The development of multifunctional nanoparticles has greatly expanded the outlook of nanomedicine with advanced imaging and therapeutic platforms. Yet the translation of these technologies will depend on a few key factors. First, the in vivo toxicity and metabolism of nanoparticles have to be addressed. As shown in current clinical trials, the nanoparticles should be either degradable or capable of being excreted through hepatic or renal pathways. Second, the nanoparticles often involve several interconnected nanocrystals and possess complex surface properties, and these features raise many concerns in terms of in vivo stability, biocompatibility, and immunogenicity. Also, new materials such as NIR QDs and upconversion nanoparticles demand longitudinal investigation of in vivo toxicity. Nevertheless, several iron oxide nanoparticles and gold nanoparticles have already shown great potential in a multifunctional regimen, which will likely shift the current paradigms of cancer intervention. The new design concepts combined with technologies that allow free integration of multiple building blocks at the nanoscale will significantly impact the development and application of multifunctional nanoparticles and contribute to the growing field of personalized medicines directed toward more accurate diagnosis and effective therapies.

Acknowledgments

This work was supported by the National Institutes of Health as an NHLBI Program of Excellence in Nanotechnology Award (HHSN268201000043C to G.B.) and an NIH Nanomedicine Development Center Award (PN2EY018244 to G.B.), by the National Science Foundation as a Science and Technology Center Grant (CBET-0939511), and by the US Department of Defense (W81XWH-11-1-0110).

LITERATURE CITED

1. Davis ME, Chen ZG, Shin DM. Nanoparticle therapeutics: an emerging treatment modality for cancer. Nat Rev Drug Discov. 2008; 7:771–82. [PubMed: 18758474]
2. Peer D, Karp JM, Hong S, Farokhzad OC, Margalit R, Langer R. Nanocarriers as an emerging platform for cancer therapy. Nat Nanotechnol. 2007; 2:751–60. [PubMed: 18654426]
3. Kim BY, Rutka JT, Chan WC. Nanomedicine. N Engl J Med. 2010; 363:2434–43. [PubMed: 21158659]

4. Hrkach J, Von Hoff D, Mukkaram Ali M, Andrianova E, Auer J, et al. Preclinical development and clinical translation of a PSMA-targeted docetaxel nanoparticle with a differentiated pharmacological profile. Sci Transl Med. 2012; 4:128ra39.
5. Gratton SE, Williams SS, Napier ME, Pohlhaus PD, Zhou Z, et al. The pursuit of a scalable nanofabrication platform for use in material and life science applications. Acc Chem Res. 2008; 41:1685–95. [PubMed: 18720952]
6. Euliss LE, DuPont JA, Gratton S, DeSimone J. Imparting size, shape, and composition control of materials for nanomedicine. Chem Soc Rev. 2006; 35:1095–104. [PubMed: 17057838]
7. Roh KH, Martin DC, Lahann J. Biphasic Janus particles with nanoscale anisotropy. Nat Mater. 2005; 4:759–63. [PubMed: 16184172]
8. Champion JA, Katare YK, Mitragotri S. Making polymeric micro- and nanoparticles of complex shapes. Proc Natl Acad Sci USA. 2007; 104:11901–4. [PubMed: 17620615]
9. Yoo JW, Irvine DJ, Discher DE, Mitragotri S. Bio-inspired, bioengineered and biomimetic drug delivery carriers. Nat Rev Drug Discov. 2011; 10:521–35. [PubMed: 21720407]
10. Petros RA, DeSimone JM. Strategies in the design of nanoparticles for therapeutic applications. Nat Rev Drug Discov. 2010; 9:615–27. [PubMed: 20616808]
11. Cleary K, Peters TM. Image-guided interventions: technology review and clinical applications. Annu Rev Biomed Eng. 2010; 12:119–42. [PubMed: 20415592]
12. Alivisatos P. The use of nanocrystals in biological detection. Nat Biotechnol. 2004; 22:47–52. [PubMed: 14704706]
13. Champion JA, Katare YK, Mitragotri S. Particle shape: a new design parameter for micro- and nanoscale drug delivery carriers. J Control Release. 2007; 121:3–9. [PubMed: 17544538]
14. Jana NR, Chen YF, Peng XG. Size- and shape-controlled magnetic (Cr, Mn, Fe, Co, Ni) oxide nanocrystals via a simple and general approach. Chem Mater. 2004; 16:3931–35.
15. Xu Z, Hou Y, Sun S. Magnetic core/shell Fe_3O_4/Au and Fe_3O_4/Au/Ag nanoparticles with tunable plasmonic properties. J Am Chem Soc. 2007; 129:8698–99. [PubMed: 17590000]
16. Popovtzer R, Agrawal A, Kotov NA, Popovtzer A, Balter J, et al. Targeted gold nanoparticles enable molecular CT imaging of cancer. Nano Lett. 2008; 8:4593–96. [PubMed: 19367807]
17. Gobin AM, Lee MH, Halas NJ, James WD, Drezek RA, West JL. Near-infrared resonant nanoshells for combined optical imaging and photothermal cancer therapy. Nano Lett. 2007; 7:1929–34. [PubMed: 17550297]
18. Hirsch LR, Stafford RJ, Bankson JA, Sershen SR, Rivera B, et al. Nanoshell-mediated near-infrared thermal therapy of tumors under magnetic resonance guidance. Proc Natl Acad Sci USA. 2003; 100:13549–54. [PubMed: 14597719]
19. Huang XH, El-Sayed IH, Qian W, El-Sayed MA. Cancer cell imaging and photothermal therapy in the near-infrared region by using gold nanorods. J Am Chem Soc. 2006; 128:2115–20. [PubMed: 16464114]
20. Doshi N, Mitragotri S. Designer biomaterials for nanomedicine. Adv Funct Mater. 2009; 19:3843–54.
21. Iqbal MA, Md S, Sahni JK, Baboota S, Dang S, Ali J. Nanostructured lipid carriers system: Recent advances in drug delivery. J Drug Target. 2012; 20:813–30. [PubMed: 22931500]
22. Peppas NA, Hilt JZ, Khademhosseini A, Langer R. Hydrogels in biology and medicine: from molecular principles to bionanotechnology. Adv Mater. 2006; 18:1345–60.
23. Liechty WB, Kryscio DR, Slaughter BV, Peppas NA. Polymers for drug delivery systems. Annu Rev Chem Biomol Eng. 2010; 1:149–73. [PubMed: 22432577]
24. Panyam J, Labhasetwar V. Biodegradable nanoparticles for drug and gene delivery to cells and tissue. Adv Drug Deliv Rev. 2003; 55:329–47. [PubMed: 12628320]
25. Vassileva ED, Koseva NS. Sonochemically born proteinaceous micro- and nanocapsules. Adv Protein Chem Struct Biol. 2010; 80:205–52. [PubMed: 21109221]
26. Hans ML, Lowman AM. Biodegradable nanoparticles for drug delivery and targeting. Curr Opin Solid State Mater Sci. 2002; 6:319–27.
27. Byrne JD, Betancourt T, Brannon-Peppas L. Active targeting schemes for nanoparticle systems in cancer therapeutics. Adv Drug Deliv Rev. 2008; 60:1615–26. [PubMed: 18840489]

28. Doiron AL, Homan KA, Emelianov S, Brannon-Peppas L. Poly (lactic-co-glycolic) acid as a carrier for imaging contrast agents. Pharm Res. 2009; 26:674–82. [PubMed: 19034628]
29. Canelas DA, Herlihy KP, DeSimone JM. Top-down particle fabrication: control of size and shape for diagnostic imaging and drug delivery. Wiley Interdiscip Rev Nanomed Nanobiotechnol. 2009; 1:391–404. [PubMed: 20049805]
30. Northfelt DW, Dezube BJ, Thommes JA, Miller BJ, Fischl MA, et al. Pegylated-liposomal doxorubicin versus doxorubicin, bleomycin, and vincristine in the treatment of AIDS-related Kaposi's sarcoma: results of a randomized phase III clinical trial. J Clin Oncol. 1998; 16:2445–51. [PubMed: 9667262]
31. Hawkins MJ, Soon-Shiong P, Desai N. Protein nanoparticles as drug carriers in clinical medicine. Adv Drug Deliv Rev. 2008; 60:876–85. [PubMed: 18423779]
32. Wang G, Uludag H. Recent developments in nanoparticle-based drug delivery and targeting systems with emphasis on protein-based nanoparticles. Expert Opin Drug Deliv. 2008; 5:499–515. [PubMed: 18491978]
33. Green MR, Manikhas GM, Orlov S, Afanasyev B, Makhson AM, et al. Abraxane®, a novel Cremophor®-free, albumin-bound particle form of paclitaxel for the treatment of advanced non-small-cell lung cancer. Ann Oncol. 2006; 17:1263–68. [PubMed: 16740598]
34. Gasco MR. Lipid nanoparticles: perspectives and challenges. Adv Drug Deliv Rev. 2007; 59:377–78. [PubMed: 17582649]
35. Oh KS, Lee KE, Han SS, Cho SH, Kim D, Yuk SH. Formation of core/shell nanoparticles with a lipid core and their application as a drug delivery system. Biomacromolecules. 2005; 6:1062–67. [PubMed: 15762679]
36. Lee CC, MacKay JA, Fréchet JMJ, Szoka FC. Designing dendrimers for biological applications. Nat Biotechnol. 2005; 23:1517–26. [PubMed: 16333296]
37. Gupta P, Vermani K, Garg S. Hydrogels: from controlled release to pH-responsive drug delivery. Drug Discov Today. 2002; 7:569–79. [PubMed: 12047857]
38. Yoo JW, Doshi N, Mitragotri S. Adaptive micro and nanoparticles: temporal control over carrier properties to facilitate drug delivery. Adv Drug Deliv Rev. 2011; 63:1247–56. [PubMed: 21605607]
39. Pridgen EM, Langer R, Farokhzad OC. Biodegradable, polymeric nanoparticle delivery systems for cancer therapy. Nanomedicine (Lond). 2007; 2:669–80. [PubMed: 17976029]
40. Caldorera-Moore M, Peppas NA. Micro- and nanotechnologies for intelligent and responsive biomaterial-based medical systems. Adv Drug Deliv Rev. 2009; 61:1391–401. [PubMed: 19758574]
41. Chilkoti A, Dreher MR, Meyer DE, Raucher D. Targeted drug delivery by thermally responsive polymers. Adv Drug Deliv Rev. 2002; 54:613–30. [PubMed: 12204595]
42. Li W, Szoka FC Jr. Lipid-based nanoparticles for nucleic acid delivery. Pharm Res. 2007; 24:438–49. [PubMed: 17252188]
43. Hook AL, Anderson DG, Langer R, Williams P, Davies MC, Alexander MR. High throughput methods applied in biomaterial development and discovery. Biomaterials. 2010; 31:187–98. [PubMed: 19815273]
44. Schroeder A, Heller DA, Winslow MM, Dahlman JE, Pratt GW, et al. Treating metastatic cancer with nanotechnology. Nat Rev Cancer. 2012; 12:39–50.
45. Boyer D, Tamarat P, Maali A, Lounis B, Orrit M. Photothermal imaging of nanometer-sized metal particles among scatterers. Science. 2002; 297:1160–63. [PubMed: 12183624]
46. Jain PK, Lee KS, El-Sayed IH, El-Sayed MA. Calculated absorption and scattering properties of gold nanoparticles of different size, shape, and composition: applications in biological imaging and biomedicine. J Phys Chem B. 2006; 110:7238–48. [PubMed: 16599493]
47. Tromberg BJ, Shah N, Lanning R, Cerussi A, Espinoza J, et al. Non-invasive in vivo characterization of breast tumors using photon migration spectroscopy. Neoplasia. 2000; 2:26–40. [PubMed: 10933066]
48. Prodan E, Radloff C, Halas NJ, Nordlander P. A hybridization model for the plasmon response of complex nanostructures. Science. 2003; 302:419–22. [PubMed: 14564001]

49. Skrabalak SE, Au L, Li XD, Xia YN. Facile synthesis of Ag nanocubes and Au nanocages. Nat Protoc. 2007; 2:2182–90. [PubMed: 17853874]
50. Halas NJ. Playing with plasmons. Tuning the optical resonant properties of metallic nanoshells. MRS Bull. 2005; 30:362–67.
51. Zharov VP, Galitovskaya EN, Johnson C, Kelly T. Synergistic enhancement of selective nanophotothermolysis with gold nanoclusters: potential for cancer therapy. Lasers Surg Med. 2005; 37:219–26. [PubMed: 16175635]
52. Jain PK, Huang XH, El-Sayed IH, El-Sayed MA. Noble metals on the nanoscale: optical and photothermal properties and some applications in imaging, sensing, biology, and medicine. Acc Chem Res. 2008; 41:1578–86. [PubMed: 18447366]
53. Qian X, Peng XH, Ansari DO, Yin-Goen Q, Chen GZ, et al. In vivo tumor targeting and spectroscopic detection with surface-enhanced Raman nanoparticle tags. Nat Biotechnol. 2008; 26:83–90. [PubMed: 18157119]
54. Yang X, Stein EW, Ashkenazi S, Wang LV. Nanoparticles for photoacoustic imaging. Wiley Interdiscip Rev Nanomed Nanobiotechnol. 2009; 1:360–68. [PubMed: 20049803]
55. Gannon CJ, Patra CR, Bhattacharya R, Mukherjee P, Curley SA. Intracellular gold nanoparticles enhance non-invasive radiofrequency thermal destruction of human gastrointestinal cancer cells. J Nanobiotechnol. 2008; 6:2.
56. von Maltzahn G, Park JH, Agrawal A, Bandaru NK, Das SK, et al. Computationally guided photothermal tumor therapy using long-circulating gold nanorod antennas. Cancer Res. 2009; 69:3892–900. [PubMed: 19366797]
57. Sun S, Zeng H, Robinson DB, Raoux S, Rice PM, et al. Monodisperse MFe_2O_4 (M = Fe, Co, Mn) nanoparticles. J Am Chem Soc. 2004; 126:273–79. [PubMed: 14709092]
58. Krishnan KM, Pakhomov AB, Bao Y, Blomqvist P, Chun Y, et al. Nanomagnetism and spin electronics: materials, microstructure and novel properties. J Mater Sci. 2006; 41:793–815.
59. Lee JH, Huh YM, Jun YW, Seo JW, Jang JT, et al. Artificially engineered magnetic nanoparticles for ultra-sensitive molecular imaging. Nat Med. 2007; 13:95–99. [PubMed: 17187073]
60. Jang JT, Nah H, Lee JH, Moon SH, Kim MG, Cheon J. Critical enhancements of MRI contrast and hyperthermic effects by dopant-controlled magnetic nanoparticles. Angew Chem Int Ed. 2009; 48:1234–38.
61. Clement O, Siauve N, Cuenod CA, Frija G. Liver imaging with ferumoxides (Feridex): fundamentals, controversies, and practical aspects. Top Magn Reson Imaging. 1998; 9:167–82. [PubMed: 9621405]
62. Tong S, Hou SJ, Zheng ZL, Zhou J, Bao G. Coating optimization of superparamagnetic iron xxide nanoparticles for high T-2 relaxivity. Nano Lett. 2010; 10:4607–13. [PubMed: 20939602]
63. Perez JM, Josephson L, O'Loughlin T, Hogemann D, Weissleder R. Magnetic relaxation switches capable of sensing molecular interactions. Nat Biotechnol. 2002; 20:816–20. [PubMed: 12134166]
64. Park JH, von Maltzahn G, Zhang L, Schwartz MP, Ruoslahti E, et al. Magnetic iron oxide nanoworms for tumor targeting and imaging. Adv Mater. 2008; 20:1630–35. [PubMed: 21687830]
65. Rosensweig RE. Heating magnetic fluid with alternating magnetic field. J Magn Magn Mater. 2002; 252:370–74.
66. Fortin JP, Wilhelm C, Servais J, Menager C, Bacri JC, Gazeau F. Size-sorted anionic iron oxide nanomagnets as colloidal mediators for magnetic hyperthermia. J Am Chem Soc. 2007; 129:2628–35. [PubMed: 17266310]
67. Lee JH, Jang JT, Choi JS, Moon SH, Noh SH, et al. Exchange-coupled magnetic nanoparticles for efficient heat induction. Nat Nanotechnol. 2011; 6:418–22. [PubMed: 21706024]
68. Dames P, Gleich B, Flemmer A, Hajek K, Seidl N, et al. Targeted delivery of magnetic aerosol droplets to the lung. Nat Nanotechnol. 2007; 2:495–99. [PubMed: 18654347]
69. Namiki Y, Namiki T, Yoshida H, Ishii Y, Tsubota A, et al. A novel magnetic crystal-lipid nano-structure for magnetically guided in vivo gene delivery. Nat Nanotechnol. 2009; 4:598–606. [PubMed: 19734934]
70. Stanley SA, Gagner JE, Damanpour S, Yoshida M, Dordick JS, Friedman JM. Radio-wave heating of iron oxide nanoparticles can regulate plasma glucose in mice. Science. 2012; 336:604–8. [PubMed: 22556257]

71. Cho MH, Lee EJ, Son M, Lee JH, Yoo D, et al. A magnetic switch for the control of cell death signalling in in vitro and in vivo systems. Nat Mater. 2012; 11:1038–43. [PubMed: 23042417]
72. Alivisatos AP, Gu W, Larabell C. Quantum dots as cellular probes. Annu Rev Biomed Eng. 2005; 7:55–76. [PubMed: 16004566]
73. Medintz IL, Uyeda HT, Goldman ER, Mattoussi H. Quantum dot bioconjugates for imaging, labelling and sensing. Nat Mater. 2005; 4:435–46. [PubMed: 15928695]
74. Hong G, Robinson JT, Zhang Y, Diao S, Antaris AL, et al. In vivo fluorescence imaging with Ag_2S quantum dots in the second near-infrared region. Angew Chem Int Ed. 2012; 51:9818–21.
75. Wang F, Han Y, Lim CS, Lu YH, Wang J, et al. Simultaneous phase and size control of upconversion nanocrystals through lanthanide doping. Nature. 2010; 463:1061–65. [PubMed: 20182508]
76. Auzel F. Upconversion and anti-Stokes processes with f and d ions in solids. Chem Rev. 2004; 104:139–74. [PubMed: 14719973]
77. Wang F, Liu X. Upconversion multicolor fine-tuning: visible to near-infrared emission from lanthanide-doped $NaYF_4$ nanoparticles. J Am Chem Soc. 2008; 130:5642–43. [PubMed: 18393419]
78. Idris NM, Gnanasammandhan MK, Zhang J, Ho PC, Mahendran R, Zhang Y. In vivo photodynamic therapy using upconversion nanoparticles as remote-controlled nanotransducers. Nat Med. 2012; 18:1580–85. [PubMed: 22983397]
79. Piao Y, Burns A, Kim J, Wiesner U, Hyeon T. Designed fabrication of silica-based nanostructured particle systems for nanomedicine applications. Adv Funct Mater. 2008; 18:3745–58.
80. Epple M, Ganesan K, Heumann R, Klesing J, Kovtun A, et al. Application of calcium phosphate nanoparticles in biomedicine. J Mater Chem. 2010; 20:18–23.
81. Maggiorella L, Barouch G, Devaux C, Pottier A, Deutsch E, et al. Nanoscale radiotherapy with hafnium oxide nanoparticles. Future Oncol. 2012; 8:1167–81. [PubMed: 23030491]
82. Larson DR, Ow H, Vishwasrao HD, Heikal AA, Wiesner U, Webb WW. Silica nanoparticle architecture determines radiative properties of encapsulated fluorophores. Chem Mater. 2008; 20:2677–84.
83. Barth BM, Sharma R, Altinoglu EI, Morgan TT, Shanmugavelandy SS, et al. Bioconjugation of calcium phosphosilicate composite nanoparticles for selective targeting of human breast and pancreatic cancers in vivo. ACS Nano. 2010; 4:1279–87. [PubMed: 20180585]
84. Liong M, Lu J, Kovochich M, Xia T, Ruehm SG, et al. Multifunctional inorganic nanoparticles for imaging, targeting, and drug delivery. ACS Nano. 2008; 2:889–96. [PubMed: 19206485]
85. Scott AW, Tyler BM, Masi BC, Upadhyay UM, Patta YR, et al. Intracranial microcapsule drug delivery device for the treatment of an experimental gliosarcoma model. Biomaterials. 2011; 32:2532–39. [PubMed: 21220172]
86. Soppimath KS, Aminabhavi TM, Kulkarni AR, Rudzinski WE. Biodegradable polymeric nanoparticles as drug delivery devices. J Control Release. 2001; 70:1–20. [PubMed: 11166403]
87. Cheng J, Teply BA, Sherifi I, Sung J, Luther G, et al. Formulation of functionalized PLGA–PEG nanoparticles for in vivo targeted drug delivery. Biomaterials. 2007; 28:869–76. [PubMed: 17055572]
88. MacEwan SR, Callahan DJ, Chilkoti A. Stimulus-responsive macromolecules and nanoparticles for cancer drug delivery. Nanomedicine (Lond). 2010; 5:793–806. [PubMed: 20662649]
89. Peppas NA. Drug delivery using smart polymers: recent advances. In: Galaev I, Mattiasson B, editorsSmart Polymers: Applications in Biotechnology And Biomedicine. Boca Raton, FL: CRC; 2007. 331–58.
90. Schmaljohann D. Thermo- and pH-responsive polymers in drug delivery. Adv Drug Deliv Rev. 2006; 58:1655–70. [PubMed: 17125884]
91. Geest BGD, Sanders NN, Sukhorukov GB, Demeester J, Smedt SCD. Release mechanisms for polyelectrolyte capsules. Chem Soc Rev. 2007; 36:636–49. [PubMed: 17387411]
92. Heffernan MJ, Murthy N. Polyketal nanoparticles: a new pH-sensitive biodegradable drug delivery vehicle. Bioconjug Chem. 2005; 16:1340–42. [PubMed: 16287226]

93. Cammas S, Suzuki K, Sone C, Sakurai Y, Kataoka K, Okano T. Thermo-responsive polymer nanoparticles with a core-shell micelle structure as site-specific drug carriers. J Control Release. 1997; 48:157–64.
94. Sershen SR, Westcott SL, Halas NJ, West JL. Temperature-sensitive polymer-nanoshell composites for photothermally modulated drug delivery. J Biomed Mater Res. 2000; 51:293–98. [PubMed: 10880069]
95. Qu LH, Peng ZA, Peng XG. Alternative routes toward high quality CdSe nanocrystals. Nano Lett. 2001; 1:333–37.
96. Hyeon T, Park J, An KJ, Hwang YS, Park JG, et al. Ultra-large-scale syntheses of monodisperse nanocrystals. Nat Mater. 2004; 3:891–95. [PubMed: 15568032]
97. Xie J, Xu C, Kohler N, Hou Y, Sun S. Controlled PEGylation of monodisperse Fe_3O_4 nanoparticles for reduced non-specific uptake by macrophage cells. Adv Mater. 2007; 19:3163–66.
98. Lattuada M, Hatton TA. Functionalization of monodisperse magnetic nanoparticles. Langmuir. 2007; 23:2158–68. [PubMed: 17279708]
99. Smith AM, Nie S. Minimizing the hydrodynamic size of quantum dots with multifunctional multidentate polymer ligands. J Am Chem Soc. 2008; 130:11278–79. [PubMed: 18680294]
100. Gittins DI, Caruso F. Biological and physical applications of water-based metal nanoparticles synthesised in organic solution. Chemphyschem. 2002; 3:110–13. [PubMed: 12465481]
101. Pellegrino T, Manna L, Kudera S, Liedl T, Koktysh D, et al. Hydrophobic nanocrystals coated with an amphiphilic polymer shell: a general route to water soluble nanocrystals. Nano Lett. 2004; 4:703–7.
102. Tong S, Hou S, Ren B, Zheng Z, Bao G. Self-assembly of phospholipid-PEG coating on nanoparticles through dual solvent exchange. Nano Lett. 2011; 11:3720–26. [PubMed: 21793503]
103. Yu WW, Chang E, Sayes CM, Drezek R, Colvin VL. Aqueous dispersion of monodisperse magnetic iron oxide nanocrystals through phase transfer. Nanotechnology. 2006; 17:4483–87.
104. Ariga K, Hill JP, Ji Q. Layer-by-layer assembly as a versatile bottom-up nanofabrication technique for exploratory research and realistic application. Phys Chem Chem Phys. 2007; 9:2319–40. [PubMed: 17492095]
105. Sinha A, Jana NR. Nanoparticle-incorporated functional mesoporous silica colloid for diverse applications. Eur J Inorg Chem. 2012; 2012:4470–78.
106. Kim J, Kim HS, Lee N, Kim T, Kim H, et al. Multifunctional uniform nanoparticles composed of a magnetite nanocrystal core and a mesoporous silica shell for magnetic resonance and fluorescence imaging and for drug delivery. Angew Chem Int Ed. 2008; 47:8438–41.
107. Park YI, Kim JH, Lee KT, Jeon KS, Bin Na H, et al. Nonblinking and nonbleaching upconverting nanoparticles as an optical imaging nanoprobe and T1 magnetic resonance imaging contrast agent. Adv Mater. 2009; 21:4467–71.
108. Wang C, Yin HF, Dai S, Sun SH. A general approach to noble metal–metal oxide dumbbell nanoparticles and their catalytic application for CO oxidation. Chem Mater. 2010; 22:3277–82.
109. Lyon JL, Fleming DA, Stone MB, Schiffer P, Williams ME. Synthesis of Fe oxide core/Au shell nanoparticles by iterative hydroxylamine seeding. Nano Lett. 2004; 4:719–23.
110. Choi JS, Lee JH, Shin TH, Song HT, Kim EY, Cheon J. Self-confirming “AND” logic nanoparticles for fault-free MRI. J Am Chem Soc. 2010; 132:11015–17. [PubMed: 20698661]
111. Jin Y, Jia C, Huang SW, O’Donnell M, Gao X. Multifunctional nanoparticles as coupled contrast agents. Nat Commun. 2010; 1:41. [PubMed: 20975706]
112. Kim J, Park S, Lee JE, Jin SM, Lee JH, et al. Designed fabrication of multifunctional magnetic gold nanoshells and their application to magnetic resonance imaging and photothermal therapy. Angew Chem Int Ed. 2006; 45:7754–58.
113. Qu HO, Ma H, Riviere A, Zhou WL, O’Connor CJ. One-pot synthesis in polyamines for preparation of water-soluble magnetite nanoparticles with amine surface reactivity. J Mater Chem. 2012; 22:3311–13.
114. Nash MA, Yager P, Hoffman AS, Stayton PS. Mixed stimuli-responsive magnetic and gold nanoparticle system for rapid purification, enrichment, and detection of biomarkers. Bioconjug Chem. 2010; 21:2197–204. [PubMed: 21070026]

115. Park JH, von Maltzahn G, Ruoslahti E, Bhatia SN, Sailor MJ. Micellar hybrid nanoparticles for simultaneous magnetofluorescent imaging and drug delivery. Angew Chem Int Ed. 2008; 47:7284–88.

116. Nasongkla N, Bey E, Ren J, Ai H, Khemtong C, et al. Multifunctional polymeric micelles as cancer-targeted, MRI-ultrasensitive drug delivery systems. Nano Lett. 2006; 6:2427–30. [PubMed: 17090068]

117. Zintchenko A, Susha AS, Concia M, Feldmann J, Wagner E, et al. Drug nanocarriers labeled with near-infrared-emitting quantum dots (quantoplexes): imaging fast dynamics of distribution in living animals. Mol Ther. 2009; 17:1849–56. [PubMed: 19707184]

118. Liu Z, Yi G, Zhang H, Ding J, Zhang Y, Xue J. Monodisperse silica nanoparticles encapsulating upconversion fluorescent and superparamagnetic nanocrystals. Chem Commun. 2008; (6):694–96.

119. Benezra M, Penate-Medina O, Zanzonico PB, Schaer D, Ow H, et al. Multimodal silica nanoparticles are effective cancer-targeted probes in a model of human melanoma. J Clin Invest. 2011; 121:2768–80. [PubMed: 21670497]

120. Xie J, Chen K, Huang J, Lee S, Wang JH, et al. PET/NIRF/MRI triple functional iron oxide nanoparticles. Biomaterials. 2010; 31:3016–22. [PubMed: 20092887]

121. Jain TK, Richey J, Strand M, Leslie-Pelecky DL, Flask CA, Labhasetwar V. Magnetic nanoparticles with dual functional properties: drug delivery and magnetic resonance imaging. Biomaterials. 2008; 29:4012–21. [PubMed: 18649936]

122. Lai CY, Trewyn BG, Jeftinija DM, Jeftinija K, Xu S, et al. A mesoporous silica nanosphere-based carrier system with chemically removable CdS nanoparticle caps for stimuli-responsive controlled release of neurotransmitters and drug molecules. J Am Chem Soc. 2003; 125:4451–59. [PubMed: 12683815]

123. Mal NK, Fujiwara M, Tanaka Y. Photocontrolled reversible release of guest molecules from coumarin-modified mesoporous silica. Nature. 2003; 421:350–53. [PubMed: 12540896]

124. Bharali DJ, Klejbor I, Stachowiak EK, Dutta P, Roy I, et al. Organically modified silica nanoparticles: a nonviral vector for in vivo gene delivery and expression in the brain. Proc Natl Acad Sci USA. 2005; 102:11539–44. [PubMed: 16051701]

125. Radu DR, Lai CY, Jeftinija K, Rowe EW, Jeftinija S, Lin VSY. A polyamidoamine dendrimer-capped mesoporous silica nanosphere-based gene transfection reagent. J Am Chem Soc. 2004; 126:13216–17. [PubMed: 15479063]

126. Juliano RL, Stamp D. The effect of particle size and charge on the clearance rates of liposomes and liposome encapsulated drugs. Biochem Biophys Res Commun. 1975; 63:651–58. [PubMed: 1131256]

127. Stolnik S, Illum L, Davis SS. Long circulating microparticulate drug carriers. Adv Drug Deliv Rev. 1995; 16:195–214.

128. Moghimi SM, Hunter AC, Murray JC. Long-circulating and target-specific nanoparticles: theory to practice. Pharm Rev. 2001; 53:283–318. [PubMed: 11356986]

129. Moghimi S, Hunter A. Poloxamers and poloxamines in nanoparticle engineering and experimental medicine. Trends Biotechnol. 2000; 18:412–20. [PubMed: 10998507]

130. Arap W, Pasqualini R, Ruoslahti E. Cancer treatment by targeted drug delivery to tumor vasculature in a mouse model. Science. 1998; 279:377–80. [PubMed: 9430587]

131. Ruoslahti E, Bhatia SN, Sailor MJ. Targeting of drugs and nanoparticles to tumors. J Cell Biol. 2010; 188:759–68. [PubMed: 20231381]

132. Farokhzad OC, Cheng J, Teply BA, Sherifi I, Jon S, et al. Targeted nanoparticle-aptamer bioconjugates for cancer chemotherapy in vivo. Proc Natl Acad Sci USA. 2006; 103:6315–20. [PubMed: 16606824]

133. Pangburn TO, Petersen MA, Waybrant B, Adil MM, Kokkoli E. Peptide- and aptamer-functionalized nanovectors for targeted delivery of therapeutics. J Biomech Eng. 2009; 131:074005. [PubMed: 19655996]

134. Barbas AS, Mi J, Clary BM, White RR. Aptamer applications for targeted cancer therapy. Future Oncol. 2010; 6:1117–26. [PubMed: 20624124]

135. Sudimack J, Lee RJ. Targeted drug delivery via the folate receptor. Adv Drug Deliv Rev. 2000; 41:147–62. [PubMed: 10699311]

136. Mi Y, Liu X, Zhao J, Ding J, Feng SS. Multimodality treatment of cancer with herceptin conjugated, thermomagnetic iron oxides and docetaxel loaded nanoparticles of biodegradable polymers. Biomaterials. 2012; 33:7519–29. [PubMed: 22809649]

137. Gu F, Zhang L, Teply BA, Mann N, Wang A, et al. Precise engineering of targeted nanoparticles by using self-assembled biointegrated block copolymers. Proc Natl Acad Sci USA. 2008; 105:2586–91. [PubMed: 18272481]

138. Roh KH, Martin DC, Lahann J. Triphasic nanocolloids. J Am Chem Soc. 2006; 128:6796–7. [PubMed: 16719453]

139. Beningo K, Wang Y. Fc-receptor-mediated phagocytosis is regulated by mechanical properties of the target. J Cell Sci. 2002; 115:849–56. [PubMed: 11865040]

140. Gratton SEA, Ropp PA, Pohlhaus PD, Luft JC, Madden VJ, et al. The effect of particle design on cellular internalization pathways. Proc Natl Acad Sci USA. 2008; 105:11613–18. [PubMed: 18697944]

141. Geng Y, Dalhaimer P, Cai S, Tsai R, Tewari M, et al. Shape effects of filaments versus spherical particles in flow and drug delivery. Nat Nanotechnol. 2007; 2:249–55. [PubMed: 18654271]

142. Champion JA, Mitragotri S. From the cover: role of target geometry in phagocytosis. Proc Natl Acad Sci USA. 2006; 103:4930–34. [PubMed: 16549762]

143. Champion JA, Mitragotri S. Shape induced inhibition of phagocytosis of polymer particles. Pharm Res. 2009; 26:244–49. [PubMed: 18548338]

144. Decuzzi P, Godin B, Tanaka T, Lee SY, Chiappini C, et al. Size and shape effects in the biodistribution of intravascularly injected particles. J Control Release. 141:320–27.

145. Decuzzi P, Ferrari M. The adhesive strength of non-spherical particles mediated by specific interactions. Biomaterials. 2006; 27:5307–14. [PubMed: 16797691]

146. Decuzzi P, Gentile F, Granaldi A, Curcio A, Causa F, et al. Flow chamber analysis of size effects in the adhesion of spherical particles. Int J Nanomed. 2007; 2:689–96.

147. Yin Y, Lu Y, Gates B, Xia Y. Template-assisted self-assembly: a practical route to complex aggregates of monodispersed colloids with well-defined sizes, shapes, and structures. J Am Chem Soc. 2001; 123:8718–29. [PubMed: 11535076]

148. Dendukuri D, Pregibon D, Collins J, Hatton T, Doyle P. Continuous-flow lithography for high-throughput microparticle synthesis. Nat Mater. 2006; 5:365–69. [PubMed: 16604080]

149. Rolland JP, Maynor BW, Euliss LE, Exner AE, Denison GM, DeSimone JM. Direct fabrication and harvesting of monodisperse, shape-specific nanobiomaterials. J Am Chem Soc. 2005; 127:10096–100. [PubMed: 16011375]

150. Lee KJ, Yoon J, Lahann J. Recent advances with anisotropic particles. Curr Opin Colloid Interface Sci. 2011; 16:195–202.

151. Cunningham CH, Arai T, Yang PC, McConnell MV, Pauly JM, Conolly SM. Positive contrast magnetic resonance imaging of cells labeled with magnetic nanoparticles. Magn Reson Med. 2005; 53:999–1005. [PubMed: 15844142]

152. Zurkiya O, Hu XP. Off-resonance saturation as a means of generating contrast with superparamagnetic nanoparticles. Magnet Reson Med. 2006; 56:726–32.

153. Shin JM, Anisur RM, Ko MK, Im GH, Lee JH, Lee IS. Hollow manganese oxide nanoparticles as multifunctional agents for magnetic resonance imaging and drug delivery. Angew Chem Int Ed. 2009; 48:321–24.

154. Harisinghani MG, Barentsz J, Hahn PF, Deserno WM, Tabatabaei S, et al. Noninvasive detection of clinically occult lymph-node metastases in prostate cancer. N Engl J Med. 2003; 348:2491–99. [PubMed: 12815134]

155. Zhao M, Beauregard DA, Loizou L, Davletov B, Brindle KM. Non-invasive detection of apoptosis using magnetic resonance imaging and a targeted contrast agent. Nat Med. 2001; 7:1241–44. [PubMed: 11689890]

156. Ghosh D, Lee Y, Thomas S, Kohli AG, Yun DS, et al. M13-templated magnetic nanoparticles for targeted in vivo imaging of prostate cancer. Nat Nanotechnol. 2012; 7:677–82. [PubMed: 22983492]

157. Fan K, Cao C, Pan Y, Lu D, Yang D, et al. Magnetoferritin nanoparticles for targeting and visualizing tumour tissues. Nat Nanotechnol. 2012; 7:459–64. [PubMed: 22706697]
158. Nahrendorf M, Jaffer FA, Kelly KA, Sosnovik DE, Aikawa E, et al. Noninvasive vascular cell adhesion molecule-1 imaging identifies inflammatory activation of cells in atherosclerosis. Circulation. 2006; 114:1504–11. [PubMed: 17000904]
159. Bruns OT, Ittrich H, Peldschus K, Kaul MG, Tromsdorf UI, et al. Real-time magnetic resonance imaging and quantification of lipoprotein metabolism in vivo using nanocrystals. Nat Nanotechnol. 2009; 4:193–201. [PubMed: 19265850]
160. Kessinger CW, Togao O, Khemtong C, Huang G, Takahashi M, Gao J. Investigation of in vivo targeting kinetics of $\alpha_V\beta_3$-specific superparamagnetic nanoprobes by time-resolved MRI. Theranostics. 2011; 1:263–73. [PubMed: 21562632]
161. Tang T, Howarth SP, Miller SR, Trivedi R, Graves MJ, et al. Assessment of inflammatory burden contralateral to the symptomatic carotid stenosis using high-resolution ultrasmall, superparamagnetic iron oxide-enhanced MRI. Stroke. 2006; 37:2266–70. [PubMed: 16917091]
162. Lewin M, Carlesso N, Tung CH, Tang XW, Cory D, et al. Tat peptide-derivatized magnetic nanoparticles allow in vivo tracking and recovery of progenitor cells. Nat Biotechnol. 2000; 18:410–14. [PubMed: 10748521]
163. Thu MS, Bryant LH, Coppola T, Jordan EK, Budde MD, et al. Self-assembling nanocomplexes by combining ferumoxytol, heparin and protamine for cell tracking by magnetic resonance imaging. Nat Med. 2012; 18:463–67. [PubMed: 22366951]
164. Barnett BP, Arepally A, Karmarkar PV, Qian D, Gilson WD, et al. Magnetic resonance-guided, real-time targeted delivery and imaging of magnetocapsules immunoprotecting pancreatic islet cells. Nat Med. 2007; 13:986–91. [PubMed: 17660829]
165. Sevick-Muraca EM. Translation of near-infrared fluorescence imaging technologies: emerging clinical applications. Annu Rev Med. 2012; 63:217–31. [PubMed: 22034868]
166. Kim S, Lim YT, Soltesz EG, De Grand AM, Lee J, et al. Near-infrared fluorescent type II quantum dots for sentinel lymph node mapping. Nat Biotechnol. 2004; 22:93–97. [PubMed: 14661026]
167. Du Y, Xu B, Fu T, Cai M, Li F, et al. Near-infrared photoluminescent Ag_2S quantum dots from a single source precursor. J Am Chem Soc. 2010; 132:1470–71. [PubMed: 20078056]
168. Xiong L, Chen Z, Tian Q, Cao T, Xu C, Li F. High contrast upconversion luminescence targeted imaging in vivo using peptide-labeled nanophosphors. Anal Chem. 2009; 81:8687–94. [PubMed: 19817386]
169. Cheng L, Yang K, Shao M, Lee ST, Liu Z. Multicolor in vivo imaging of upconversion nanoparticles with emissions tuned by luminescence resonance energy transfer. J Phys Chem C. 2011; 115:2686–92.
170. Chen J, Saeki F, Wiley BJ, Cang H, Cobb MJ, et al. Gold nanocages: bioconjugation and their potential use as optical imaging contrast agents. Nano Lett. 2005; 5:473–77. [PubMed: 15755097]
171. Zhang HF, Maslov K, Stoica G, Wang LV. Functional photoacoustic microscopy for high-resolution and noninvasive in vivo imaging. Nat Biotechnol. 2006; 24:848–51. [PubMed: 16823374]
172. Wang Y, Xie X, Wang X, Ku G, Gill KL, et al. Photoacoustic tomography of a nanoshell contrast agent in the in vivo rat brain. Nano Lett. 2004; 4:1689–92.
173. Yang X, Skrabalak SE, Li ZY, Xia Y, Wang LV. Photoacoustic tomography of a rat cerebral cortex in vivo with Au nanocages as an optical contrast agent. Nano Lett. 2007; 7:3798–802. [PubMed: 18020475]
174. Mallidi S, Larson T, Aaron J, Sokolov K, Emelianov S. Molecular specific optoacoustic imaging with plasmonic nanoparticles. Opt Express. 2007; 15:6583–88. [PubMed: 19546967]
175. Li PC, Wei CW, Liao CK, Chen CD, Pao KC, et al. Photoacoustic imaging of multiple targets using gold nanorods. IEEE Trans Ultrason Ferroelectr Freq Control. 2007; 54:1642–47. [PubMed: 17703668]

176. Galanzha EI, Shashkov EV, Kelly T, Kim JW, Yang L, Zharov VP. In vivo magnetic enrichment and multiplex photoacoustic detection of circulating tumour cells. Nat Nanotechnol. 2009; 4:855–60. [PubMed: 19915570]

177. Mallidi S, Larson T, Tam J, Joshi PP, Karpiouk A, et al. Multiwavelength photoacoustic imaging and plasmon resonance coupling of gold nanoparticles for selective detection of cancer. Nano Lett. 2009; 9:2825–31. [PubMed: 19572747]

178. Kim G, Huang SW, Day KC, O'Donnell M, Agayan RR, et al. Indocyanine-green-embedded PEBBLEs as a contrast agent for photoacoustic imaging. J Biomed Opt. 2007; 12:044020. [PubMed: 17867824]

179. Pan D, Cai X, Yalaz C, Senpan A, Omanakuttan K, et al. Photoacoustic sentinel lymph node imaging with self-assembled copper neodecanoate nanoparticles. ACS Nano. 2012; 6:1260–67. [PubMed: 22229462]

180. Ku G, Zhou M, Song S, Huang Q, Hazle J, Li C. Copper sulfide nanoparticles as a new class of photoacoustic contrast agent for deep tissue imaging at 1064 nm. ACS Nano. 2012; 6:7489–96. [PubMed: 22812694]

181. Kircher MF, Mahmood U, King RS, Weissleder R, Josephson L. A multimodal nanoparticle for preoperative magnetic resonance imaging and intraoperative optical brain tumor delineation. Cancer Res. 2003; 63:8122–25. [PubMed: 14678964]

182. Lin X, Xie J, Niu G, Zhang F, Gao H, et al. Chimeric ferritin nanocages for multiple function loading and multimodal imaging. Nano Lett. 2011; 11:814–19. [PubMed: 21210706]

183. Xia A, Chen M, Gao Y, Wu D, Feng W, Li F. Gd^{3+} complex-modified $NaLuF_4$-based up-conversion nanophosphors for trimodality imaging of NIR-to-NIR upconversion luminescence, X-ray computed tomography and magnetic resonance. Biomaterials. 2012; 33:5394–405. [PubMed: 22560666]

184. Kircher MF, de la Zerda A, Jokerst JV, Zavaleta CL, Kempen PJ, et al. A brain tumor molecular imaging strategy using a new triple-modality MRI-photoacoustic-Raman nanoparticle. Nat Med. 2012; 18:829–34. [PubMed: 22504484]

185. Nahrendorf M, Zhang H, Hembrador S, Panizzi P, Sosnovik DE, et al. Nanoparticle PET-CT imaging of macrophages in inflammatory atherosclerosis. Circulation. 2008; 117:379–87. [PubMed: 18158358]

186. Lee HY, Li Z, Chen K, Hsu AR, Xu C, et al. PET/MRI dual-modality tumor imaging using arginine-glycine-aspartic (RGD)-conjugated radiolabeled iron oxide nanoparticles. J Nucl Med. 2008; 49:1371–79. [PubMed: 18632815]

187. Jain RK. Delivery of molecular and cellular medicine to solid tumors. Adv Drug Deliv Rev. 2001; 46:149–68. [PubMed: 11259838]

188. Alexis F, Rhee JW, Richie JP, Radovic-Moreno AF, Langer R, Farokhzad OC. New frontiers in nanotechnology for cancer treatment. Urol Oncol. 2008; 26:74–85. [PubMed: 18190835]

189. Wang AZ, Langer R, Farokhzad OC. Nanoparticle delivery of cancer drugs. Annu Rev Med. 2012; 63:185–98. [PubMed: 21888516]

190. Galvin P, Thompson D, Ryan KB, McCarthy A, Moore AC, et al. Nanoparticle-based drug delivery: case studies for cancer and cardiovascular applications. Cell Mol Life Sci. 2012; 69:389–404. [PubMed: 22015612]

191. Leleux J, Roy K. Micro and nanoparticle-based delivery systems for vaccine immunotherapy: an immunological and materials perspective. Adv Healthc Mater. 2013; 2:72–94. [PubMed: 23225517]

192. Cheng Z, Al Zaki A, Hui JZ, Muzykantov VR, Tsourkas A. Multifunctional nanoparticles: cost versus benefit of adding targeting and imaging capabilities. Science. 2012; 338:903–10. [PubMed: 23161990]

193. Nobuto H, Sugita T, Kubo T, Shimose S, Yasunaga Y, et al. Evaluation of systemic chemotherapy with magnetic liposomal doxorubicin and a dipole external electromagnet. Int J Cancer. 2004; 109:627–35. [PubMed: 14991586]

194. Medarova Z, Pham W, Farrar C, Petkova V, Moore A. In vivo imaging of siRNA delivery and silencing in tumors. Nat Med. 2007; 13:372–77. [PubMed: 17322898]

195. Cho NH, Cheong TC, Min JH, Wu JH, Lee SJ, et al. A multifunctional core-shell nanoparticle for dendritic cell-based cancer immunotherapy. Nat Nanotechnol. 2011; 6:675–82. [PubMed: 21909083]
196. Viglianti BL, Abraham SA, Michelich CR, Yarmolenko PS, MacFall JR, et al. In vivo monitoring of tissue pharmacokinetics of liposome/drug using MRI: illustration of targeted delivery. Magn Reson Med. 2004; 51:1153–62. [PubMed: 15170835]
197. Medarova Z, Rashkovetsky L, Pantazopoulos P, Moore A. Multiparametric monitoring of tumor response to chemotherapy by noninvasive imaging. Cancer Res. 2009; 69:1182–89. [PubMed: 19141648]
198. Furlani EP, Ng KC. Nanoscale magnetic biotransport with application to magnetofection. Phys Rev E. 2008; 77:061914.
199. Shapiro B. Towards dynamic control of magnetic fields to focus magnetic carriers to targets deep inside the body. J Magn Magn Mater. 2009; 321:1594–99. [PubMed: 20165553]
200. Yellen BB, Forbes ZG, Halverson DS, Fridman G, Barbee KA, et al. Targeted drug delivery to magnetic implants for therapeutic applications. J Magn Magn Mater. 2005; 293:647–54.
201. Widder KJ, Senyel AE, Scarpelli GD. Magnetic microspheres: a model system of site specific drug delivery in vivo. Proc Soc Exp Biol Med. 1978; 158:141–46. [PubMed: 674215]
202. Widder KJ, Morris RM, Poore GA, Howard DP, Senyei AE. Selective targeting of magnetic albumin microspheres containing low-dose doxorubicin: total remission in Yoshida sarcoma-bearing rats. Eur J Cancer Clin Oncol. 1983; 19:135–39. [PubMed: 6682771]
203. Rudge S, Peterson C, Vessely C, Koda J, Stevens S, Catterall L. Adsorption and desorption of chemotherapeutic drugs from a magnetically targeted carrier (MTC). J Control Release. 2001; 74:335–40. [PubMed: 11489515]
204. Alexiou C, Arnold W, Klein RJ, Parak FG, Hulin P, et al. Locoregional cancer treatment with magnetic drug targeting. Cancer Res. 2000; 60:6641–48. [PubMed: 11118047]
205. Chorny M, Fishbein I, Yellen BB, Alferiev IS, Bakay M, et al. Targeting stents with local delivery of paclitaxel-loaded magnetic nanoparticles using uniform fields. Proc Natl Acad Sci USA. 2010; 107:8346–51. [PubMed: 20404175]
206. Hofmann A, Wenzel D, Becher UM, Freitag DF, Klein AM, et al. Combined targeting of lentiviral vectors and positioning of transduced cells by magnetic nanoparticles. Proc Natl Acad Sci USA. 2009; 106:44–49. [PubMed: 19118196]
207. Cheng K, Malliaras K, Li TS, Sun B, Houde C, et al. Magnetic enhancement of cell retention, engraftment, and functional benefit after intracoronary delivery of cardiac-derived stem cells in a rat model of ischemia/reperfusion. Cell Transplant. 2012; 21:1121–35. [PubMed: 22405128]
208. Kong G, Braun RD, Dewhirst MW. Characterization of the effect of hyperthermia on nanoparticle extravasation from tumor vasculature. Cancer Res. 2001; 61:3027–32. [PubMed: 11306483]
209. Hu SH, Chen SY, Liu DM, Hsiao CS. Core/single-crystal-shell nanospheres for controlled drug release via a magnetically triggered rupturing mechanism. Adv Mater. 2008; 20:2690–95. [PubMed: 25213891]
210. Thomas CR, Ferris DP, Lee JH, Choi E, Cho MH, et al. Noninvasive remote-controlled release of drug molecules in vitro using magnetic actuation of mechanized nanoparticles. J Am Chem Soc. 2010; 132:10623–25. [PubMed: 20681678]
211. Derfus AM, von Maltzahn G, Harris TJ, Duza T, Vecchio KS, et al. Remotely triggered release from magnetic nanoparticles. Adv Mater. 2007; 19:3932–36.
212. Lu W, Zhang G, Zhang R, Flores LG, Huang Q, et al. Tumor site–specific silencing of NF-κB p65 by targeted hollow gold nanosphere–mediated photothermal transfection. Cancer Res. 2010; 70:3177–88. [PubMed: 20388791]

SUMMARY POINTS

1. Inorganic and organic nanoparticles have unique plasmonic, magnetic, and optical properties that can be tuned through size or composition or both. These nanoparticles have provided remarkable contrast enhancement for nearly all medical imaging modalities, in particular, MRI, photoacoustic imaging, and optical imaging. In addition, gold nanoparticles and iron oxide nanoparticles are being used as probes for thermal therapies in cancer treatment.
2. Technologies are available for integrating various nanoparticles or adding small molecule moieties to nanoparticles to form one unifying nanostructure with multiple functionalities for coupled diagnostic imaging, drug/gene delivery, and thermal therapy.
3. Nanoparticle-based multimodality imaging probes have shown great potential in multi-scale medical imaging. By combining complementary imaging capabilities, these probes improve disease characterization at multiple length scales and spatial resolutions. These integrative imaging techniques not only facilitate disease study in laboratory and clinical research but also assist treatment planning at different stages of medical interventions.
4. Inorganic nanoparticle as nanosized drug carriers can shift the paradigm of current disease treatment by implementing imaging-guided drug delivery, magnetic targeting, and combined drug delivery and thermal therapy.
5. Clinical studies have demonstrated excellent biocompatibility of several types of inorganic nanoparticles, including gold nanoparticles, iron oxide nanoparticles, and silica nanoparticles. This may further facilitate translations of multifunctional nanoparticles into clinical applications.
6. The great challenges that need to be addressed in the translations of multifunctional nanoparticles include in vivo stability, immunocompatibility, and toxicity due to increased structural and chemical complexity.

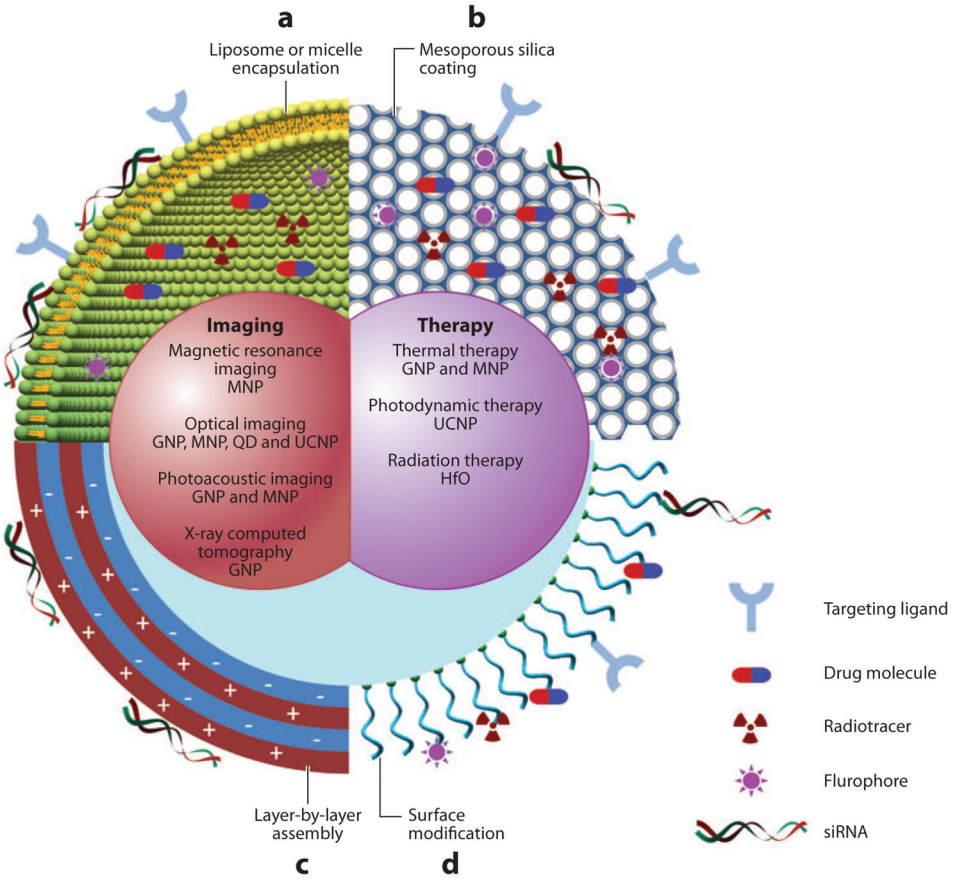

Figure 1.

Schematic diagram of multifunctional nanoparticles. Multifunctional nanoparticles can be generated by either combining nanocrystals with different functionalities or combining nanocrystals with functional small-molecule cargos through different surface engineering strategies. Four typical coatings developed for inorganic nanocrystals are (*a*) liposome or micelle encapsulation, (*b*) mesoporous silica coating, (*c*) layer-by-layer assembly, and (*d*) surface conjugation. Abbreviations: GNP, gold nanoparticles; HfO, hafnium oxide nanoparticles; MNP, magnetic nanoparticles; QD, quantum dot; UCNP, upconversion nanoparticles.

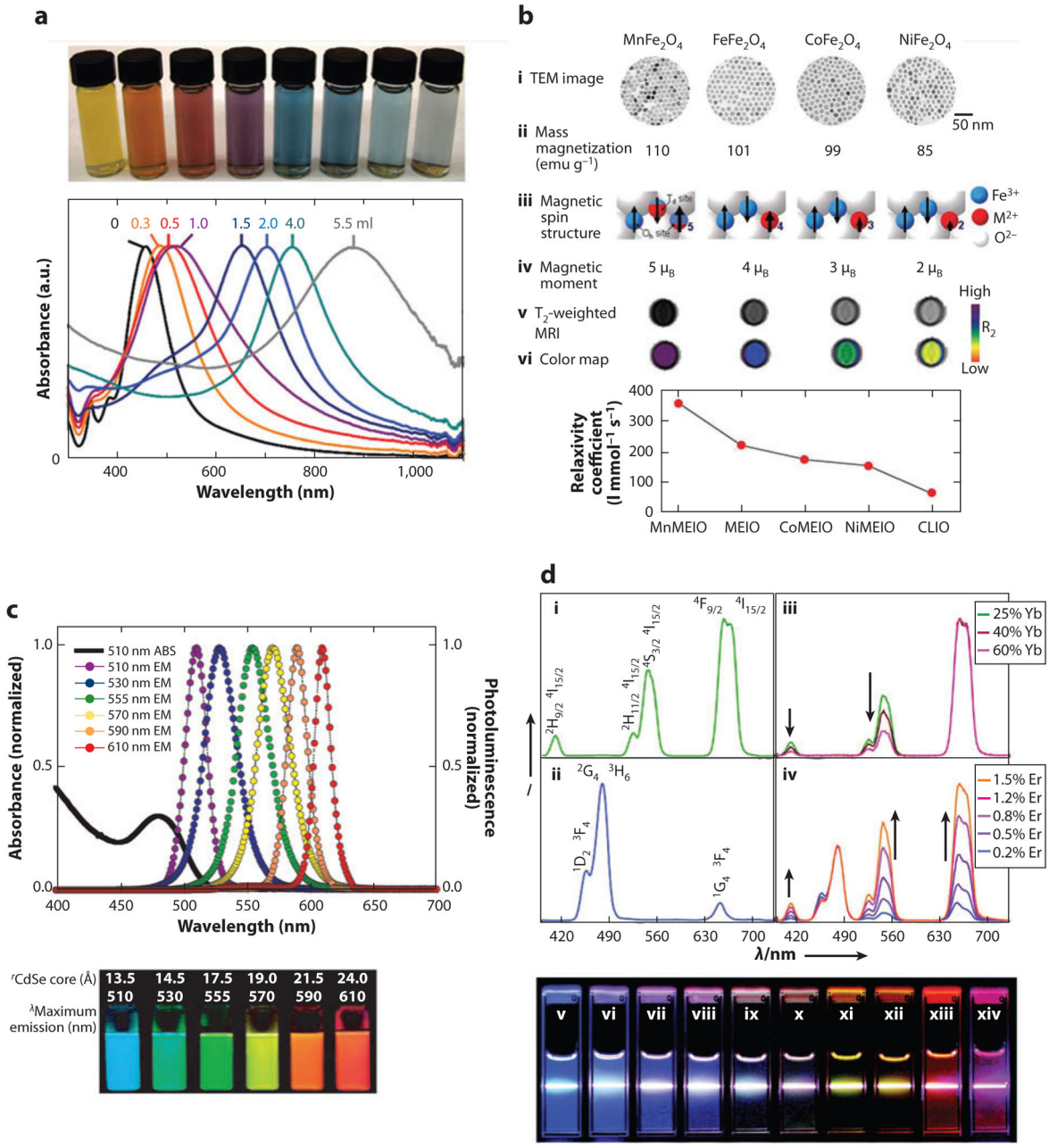

Figure 2.

Physical properties of inorganic nanoparticles. (*a*) Gold nanocage showing tunable surface plasmon resonance peak. (Reprinted from Reference 49 with permission from Macmillan Publishers Ltd ©2007.) (*b*) Magnetic nanoparticles generated by doping iron oxide with various magnetic ions. These nanoparticles exhibit different mass magnetization and, subsequently, MRI T_2 relaxivity. (Reprinted from Reference 59 with permission from Macmillan Publishers Ltd © 2007.) (*c*) Quantum dots showing size-tunable fluorescence emission. (Reprinted from Reference 73 with permission from Macmillan Publishers Ltd © 2005.) (*d*) Emission spectra of upconversion nanoparticles with different sensitizer and

activator ions. (Reprinted with permission from Reference 77, © 2008 American Chemical Society.) Abbreviations: λl, wavelength; CLIO, cross-linked iron oxide; MEIO, magnetism-engineered iron oxide; MRI, magnetic resonance imaging; TEM, transmission electron microscopy; ABS, absorption spectrum; EM, emission.

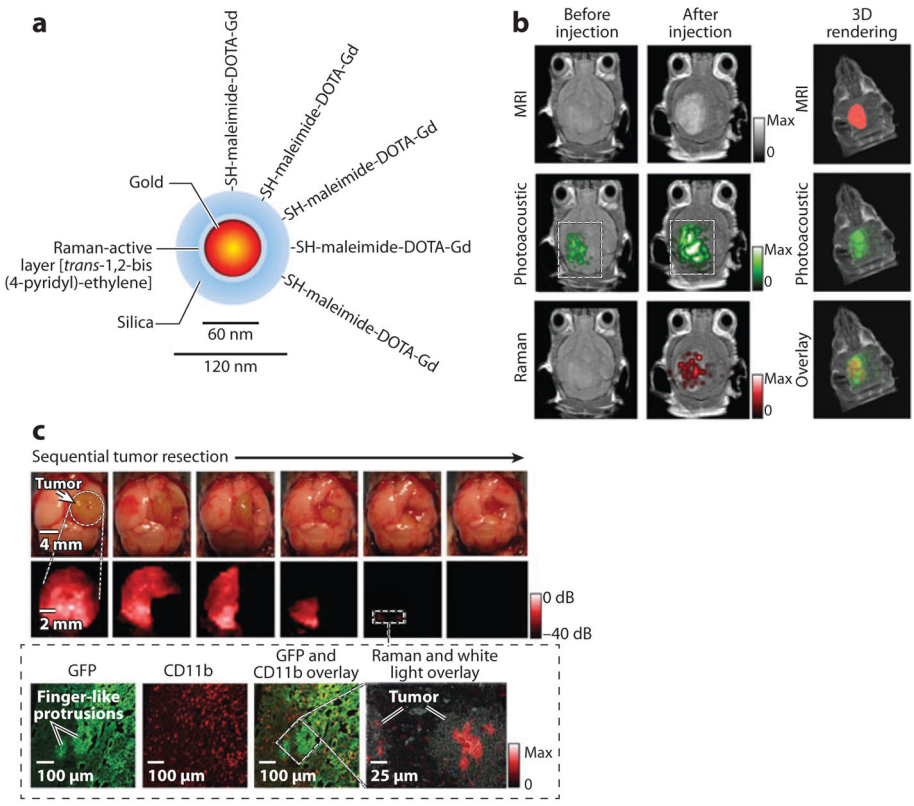

Figure 3.

Trimodality nanoparticle for pre- and intraoperative brain tumor imaging. (*a*) Trimodality detection of brain tumors in living mice. (*b*) Raman-guided intraoperative surgery. Abbreviations: CD11b, cluster of differentiation molecule 11b; GFP, green fluorescent protein; MRI, magnetic resonance imaging. (Reprinted from Reference 184 with permission from Macmillan Publishers Ltd © 2012.)

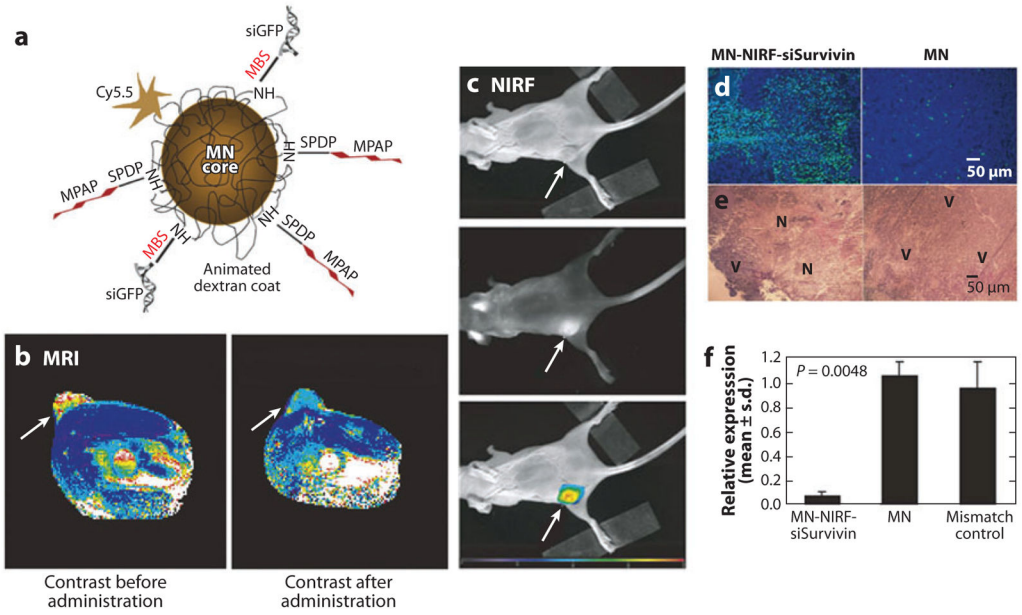

Figure 4.

Image-guided siRNA delivery. (*a*) Schematic diagram of the siRNA carrier with MRI/NIR modalities (MN-NIRF-siRNA). MN core and Cy5.5 can be detected with MRI and NIRF imaging, respectively. (*b*) In vivo MRI of mice bearing subcutaneous LS174T human colorectal adenocarcinoma (*arrows*). The significant drop in T_2 relaxivity after administration of the contrast agent (P = 0.003) confirmed probe delivery. (*c*) NIRF imaging of the mouse following injection of MN-NIRF-siSurvivin (*top*: white light, *middle*: NIRF, *bottom*: color-coded overlay). (*d*) The tumor treated with MN-NIRF-siSurvivin (*left*) showed distinct areas with a high density of apoptotic nuclei (*green*). Sections were counterstained with DAPI. (*e*) H&E staining of frozen tumor sections revealed considerable eosinophilic areas of tumor necrosis (N) in tumors treated with MN-NIRF-siSurvivin (*left*). Purple hematoxiphilic regions (V) indicate viable tumor tissues. (*f*) Quantitative RT-PCR analysis of survivin expression in LS174T tumors after injection with either MN-NIRF-siSurvivin, a mismatch control, or the parental MN. Abbreviations: DAPI, diamidino-2-phenylindole; GFP, green fluorescent protein; H&E, ematoxylin and eosin; MN, magnetic nanoparticle; MPAP, myristoylated polyarginine peptide; NIRF, near-infrared fluorescence; RT-PCR, real-time polymerase chain reaction. (Reprinted from Reference 194 with permission from Macmillan Publishers Ltd © 2007.)

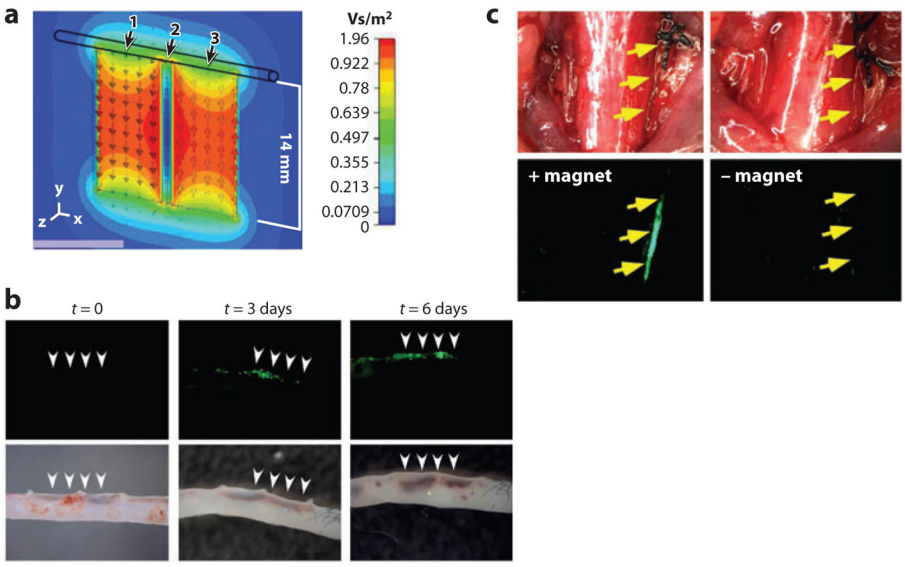

Figure 5.

Magnetic targeting of lentiviral vectors and positioning of transduced cells. (*a*) The magnetic flux density of magnets placed next to a vessel. (*b*) Magnetic targeting of lentiviral vectors to aorta during ex vivo perfusion. (*c*) In vivo positioning of lentivirus/magnetic nanoparticle–transduced HUVECs (human umbilical vein endothelial cells) to the intimae of injured common carotid arteries by magnetic forces. (Reprinted with permission from Reference 206, © 2009 National Academy of Sciences.)

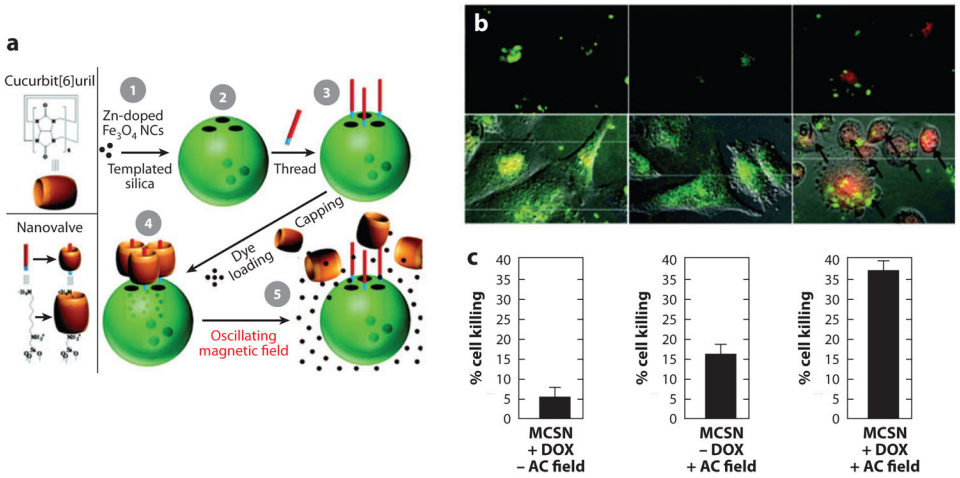

Figure 6.

Magnetically activated release system (MARS). (*a*) Schematic diagram of nanoparticles, machines, and assembly. Magnetic-core silica nanoparticles (MCSN) are synthesized by coating zinc-doped iron oxide nanocrystals (1) with mesoporous silica (2). The base of the molecular machine is then attached to the nanoparticle surface (3). The drug is loaded into the particle and capped (4) to complete the system. Release can be realized using remote heating via the introduction of an oscillating magnetic field (5). (*b*) Fluorescent microscope images (1, 3, and 5) and fluorescent images overlaid with differential interference contrast (DIC) (2, 4, and 6). Images 5 and 6 demonstrate doxorubicin (DOX) release after a 5-min AC field exposure. Color scheme: green, fluorescently labeled MARS; red, DOX; yellow, merged green and red. (*c*) Quantification of cell death after treatments shown in Panel *b*. (Reprinted with permission from Reference 210, © 2010 American Chemical Society.)

Table 1

Examples of synthesis schemes for multifunctional nanoparticles

Synthesis method	Nanoparticles	References
Nanoparticle-nanoparticle combination		
■ Seed-mediated growth	$NaGdF_4$@$NaGdF_4$:Yb^{3+}/Er^{3+}, gold shell@SPIO	15, 107
■ Metal coordination/chelation	Gold shell/silica (gold seeds are first absorbed onto silica surface through gold-amine coordination), gold nanosphere@SPIO	18, 113
■ Biological/chemical bond	Gold nanosphere and SPIO linked via biotin-streptavidin interaction. SPIO linked to silica via chemical bonds	112, 114
■ Hydrophobic/electric interaction	QD and SPIO in phospholipid-PEG, QD with negative charges in PEG-PEI	115, 117
■ Physical entrapment	Various nanoparticles entrapped in mesoporous silica or liposomes	69, 105
Nanoparticle–small molecule combination		
■ Chemical conjugation	TRITC, Cy5, and ^{124}I conjugated to C dots, Cy5.5 and ^{64}Cu-DOTA conjugated to SPIO	82, 119, 120
■ Electrostatic interaction	Plasmid DNA complexed with silica nanoparticles or mesoporous silica	124, 125
■ Hydrophobic interaction	Doxorubicin in phospholipid-PEG micelle, cholestane and phenanthrene in mesoporous silica	115, 121–123

Abbreviations: PEG, poly(ethylene glycol); PEI, poly(ethyl enimine); QD, quantum dot; SPIO, superparamagnetic iron oxide nanoparticle; TRITC, tetramethylrhodamine isothiocyanate.

Table 2

Inorganic nanoparticles on the market and in clinical trials

Commercial name	Compound	Function	Target disease	Development stage
Feridex I.V.®	Dextran-coated SPIO	MRI contrast agent	Liver tumors	FDA approval in 1996
GastroMARK™	Silicone-coated SPIO	MRI contrast agent	Gastrointestinal forms of cancer	FDA approval in 1996
Resovist®	Carboxydextrane-coated SPIO	MRI contrast agent	Liver tumors	EU approval in 2001
Acticoat	Silver nanoparticles	Antimicrobial barrier dressing	Wound healing	FDA approval in 2005
NanoTherm	Aminosilane-coated SPIO	Magnetic thermotherapy	Brain tumors Prostate and pancreatic carcinoma	EU approval in 2010 Phase I
NBTXR3	Hafnium oxide nanoparticle	Radiation therapy	Soft-tissue sarcoma	Phase 1
-	Silica-gold nanoparticles	Photothermal ablation of atherosclerotic plaques	Atherosclerosis	Phase 1/phase 2
AuroShell®	Gold@silica nanoshells	Photothermal therapy	Refractory head and neck cancers Primary and metastatic tumors in the lung	Phase 1 Approved by FDA for clinical trials in 2012
Aurimmune	TNF-α-bound PEGylated colloidal gold particles	Targeted delivery of TNF-α	Solid tumors	Completed phase 1
Cornell dots	Silica nanoparticles embedded with fluorophores or radioactive iodine	Fluorescence/PET contrast agents	Cancer	Approved by FDA for clinical trials in 2011

Abbreviations: FDA, US Food and Drug Administration; PET, positron emission tomography; phase 1/2, clinical trial phases; SPIO, superparamagnetic iron oxide nanoparticle; TNF, tumor necrosis factor.